A NEARLY LINEAR

CIRCUIT MODEL FOR THE PIN DIODE

by

GIM POY HOM

S.B., MASSACHUSETTS INSTITUTE OF TECHNOLOGY
February, 1971

SUBMITTED IN PARTIAL FULFILLMENT OF THE

REQUIREMENTS FOR THE DEGREE OF

MASTER OF SCIENCE

at the

MASSACHUSETTS INSTITUTE OF TECHNOLOGY
August, 1972

Signature of Author _____
Department of Electrical Engineering
August 14, 1972

Certified by _____
Thesis Supervisor

Accepted by _____
Chairman, Departmental Committee
on Graduate Students

A NEARLY LINEAR CIRCUIT MODEL FOR THE PIN DIODE

by

GIM POY HOM

Submitted to the Department of Electrical Engineering on 14 August, 1972 in partial fulfillment of the requirements for the degree of Master of Science.

ABSTRACT

The potential applicability of semiconductor diodes in RF and microwave switching circuits is limited by the distortion produced by the incremental non-linearity of such devices. The incremental non-linearity of PIN diodes is significantly lower than that of other diode types at high frequencies because of the long minority carrier lifetimes commonly found in the PIN structures. It is desirable to characterize the distortion producing mechanisms in PIN structures in order to establish performance limits both in terms of frequency and in terms of power handling capability. Frequency and power level dependent relationships between diode parameters such as minority carrier lifetime, doping profile, junction area, etc.,and the resulting distortion observed in simple RF circuit applications are derived, thus establishing theoretical performance limits of the diodes. Measured distortion levels in the diodes agree with the theoretical predictions in most cases.

Thesis Supervisor: Donald H. Steinbrecher

Title: Associate Professor of Electrical Engineering

ACKNOWLEDGEMENT

I would like to thank my thesis advisor, Professor Donald H. Steinbrecher for his help and guidance, and most of all, for being more than just a thesis advisor.

Sincere thanks also to Dr. A. Carlson and Tony De Christoforos of Varian and Dr. P. Chorney of Unitrode for providing the PIN diodes for the experiment; to Professor R. Adler for the informative chats, and to Ms. M.C. Cheung for typing the manuscript.

Table of Contents

		page
Section I	Introduction	5
Section II	PIN Diode Semiconductor Physics	
	2.0 Introduction	7
	2.1 DC Analysis	8
	2.2 AC Analysis	14
	2.3 Power Handling Capabilities	17
Section III	Non-Linearities in the PIN Diode	
	3.0 Introduction	19
	3.1 Linear Resistance Method (Harmonic Products)	20
	3.2 Fourier Series Method (Harmonic Products)	21
	3.3 Linear Resistance Method (Intermodulation Products)	25
	3.4 Fourier Series Method (Intermodulation Products)	27
Section IV	Intermodulation Product Measurement	
	4.0 Introduction	31
	4.1 Theoretical Calculations of Third Order Intercept	38
	4.2 Measured Results	39
Section V	Conclusion	58
Appendix A	Intermodulation Distortion Analysis	59
Appendix B	List of Symbols	62
References		63
Other References		64

I Introduction

PIN diodes find many applications in microwave switch attenuators and phase shifters. PIN structures are very similar to PNPN, PNIN, and other semiconductor diodes. Theoretical analysis of these devices can be found in the literature. [1] [2] [3] But to the best of the author's knowledge, little has been done to determine a nearly linear circuit model that can be used to predict distortion levels resulting from PIN diodes in RF circuits. The characterization of the distortion, and in particular, intermodulation distortion in PIN diodes has been done empirically. [4] With a nearly linear circuit model of the PIN diode circuit elements a function of the physical parameters, theoretical limits on intermodulation distortion can now be predicted. Hence the fundamental limit in, say a high dynamic range switch, can be derived theoretically.

It is ironic that the characteristic that makes PIN diodes desirable in microwave application also makes their characterization difficult: that is, their very low distortion levels. It is not uncommon to find the harmonic content of the PIN's to be 50 - 120 db below the fundamental. However, using a cancellation scheme designed and built by D.H. Steinbrecher and R. Mohlere, [5] it is possible to detect inband intermodulation products as low as 110 db below the primary test frequencies.

In Section II, the semiconductor physics of the PIN diode is given along with a nearly linear circuit model. Using this model, theoretical harmonic and intermodulation product

levels can be derived. The reults are given in Section III.

Comparison of measured third order intermodulation product levels, using the cancellation unit, and theoretical predictions were made. From the data, it appears that the theoretical model gives the proper third order product frequency dependent relations. However, there is a significant error in the current dependent relations.

In deriving a circuit model, it was assumed that the I region width and the carrier lifetime are both independent of the current level; actually, they are not. Increasing current tends to decrease carrier lifetime and increase the I region width, thereby increasing the harmonic and intermodulation product levels. This is one possible explanation for the errors in current dependence. Others might be the approximations used in calculating the I region resistance. If exact expressions were used, it would not have been possible to calculate the I region resistance in closed form.

It appears that if the current dependent relationship of the I region width and carrier lifetime can be determined, then the non-linearities in the PIN diode can then be fully characterized.

II PIN Semiconductor Physics

2.0 Introduction

The PIN structure is a triple-layer doubly-diffused semiconductor device consisting of a P-doped region, an intrinsic region and an N-doped region. The high resistivity I region is generally between 10 - 100 microns thick.

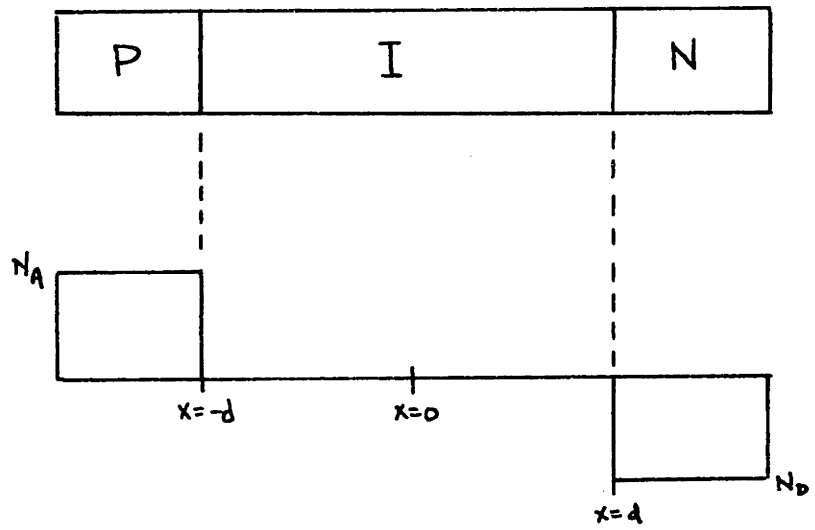

Figure 2.1 PIN Diode

The first PIN structure was proposed by R.N. Hall, [6] not as a high frequency device, but as a high voltage rectifier because the presence of an I region greatly increases the reverse breakdown voltage. Late in 1958, [7] it was discovered that the PIN diode behaved as a very linear resistance at microwave frequencies. This I region resistance, dependent only on DC bias, can be varied from thousands of ohms, under zero or reverse bias, to a fraction of an ohm under heavy forward bias.

Figure 2.2 is an application of a PIN diode as a shunt switch.

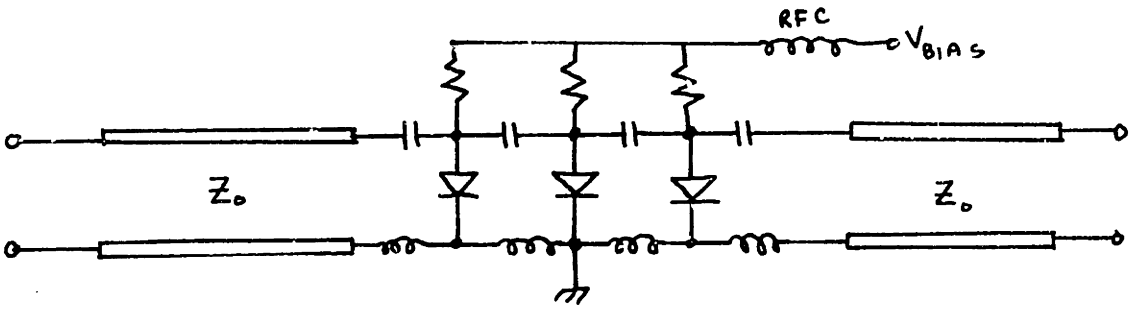

Figure 2.2 PIN Diode Shunt Switch

The presence of stored charges in the I region also permits a higher power-level capability than ordinary PN diode. This will be discussed in Section 2.3.

2.1 D.C. Analysis

In deriving a nearly linear circuit model it is necessary to analyze the semiconductor physics of the device. Though an exact analysis will yield a good characterization of the minority carrier profile in the intrinsic region, we must resort to an approximation of the carrier profile in order to arrive at a reasonable circuit model of the PIN with element values in closed form.

In forward bias application of the PIN diode, the current density J will no longer satisfy the low level injection condition, therefore, an analysis under high level injection will be given. [8], *

---

* The semiconductor physics in this section was derived by A. Kokkas, Massachusetts Institute of Technology.

Charge neutrality condition:

(2.1) $$n - p = N_d - N_a = N$$

Time dependent diffusion equations:

(2.2) $$J = J_h + J_e$$

(2.3) $$J_h = q\mu_h\left[pE - \frac{kT}{q}\frac{\partial p}{\partial x}\right]$$

(2.4) $$J_e = q\mu_e\left[nE + \frac{kT}{q}\frac{\partial n}{\partial x}\right]$$

(2.5) $$\frac{\partial J_h}{\partial x} = -q\frac{p-p_0}{\tau} - q\frac{\partial p}{\partial t}$$

Eliminating all variables from equations (2.1)-(2.5) we get:

(2.6) $$\frac{\partial^2 p}{\partial x^2} + \frac{(b-1)N}{(2p+N)[(b+1)p+bN]}\left(\frac{\partial p}{\partial x}\right)^2 - \frac{JN}{qD_h(2p+N)[(b+1)p+bN]}\frac{\partial p}{\partial x}$$

$$-\frac{(b+1)p+bN}{(2p+N)b}\frac{p-p_0}{L_h^2} = \frac{(b+1)p+bN}{D_h(2p+N)b}\frac{\partial p}{\partial t} \qquad b = \mu_e/\mu_h$$

For high level injection; we get:

(2.7) $$\frac{\partial^2 p}{\partial x^2} - \frac{p-p_0}{L_a^2} = \frac{1}{D_a}\frac{\partial p}{\partial t}, \quad L_a = L_h\sqrt{2b/b+1}$$

Solving for $\frac{\partial p}{\partial x}$ in (2.2), (2.3), and (2.4):

(2.8) $$\frac{\partial p}{\partial x} = \frac{p\mu_h J_e - (p+N)\mu_e J_n}{\mu_e \mu_h kT (2p+N)}$$

Now, under high level injection, J at x = +d will be majority carrier current only, i.e.:

$$J(x=d) = J_e$$

A similar argument holds for J(-d). Thus, we get the boundary conditions at high level injection.

(2.9) $$\left.\frac{\partial p}{\partial x}\right|_{x=-d} = \frac{-J}{2\mu_h kT}$$

(2.10) $$\left.\frac{\partial p}{\partial x}\right|_{x=d} = \frac{J}{2\mu_e kT}$$

When equation (2.7) is solved, subject to the above boundary conditions, we get:

(2.11) $$p(x) - p_o = \frac{J L_a}{2kT \sinh\frac{2d}{L_a}}\left[\frac{1}{\mu_e}\cosh\left(\frac{x+d}{L_a}\right) + \frac{1}{\mu_h}\cosh\left(\frac{x-d}{L_a}\right)\right]$$

p(x) is plotted as a function of x in Figure 2.3 using:

$I = 20$ ma

$A = 10^{-4}$ cm^2

$L_a = 2.5 \times 10^{-3}$ cm

$\mu_e = 3\mu_h = 1350$ cm^2/volt-sec

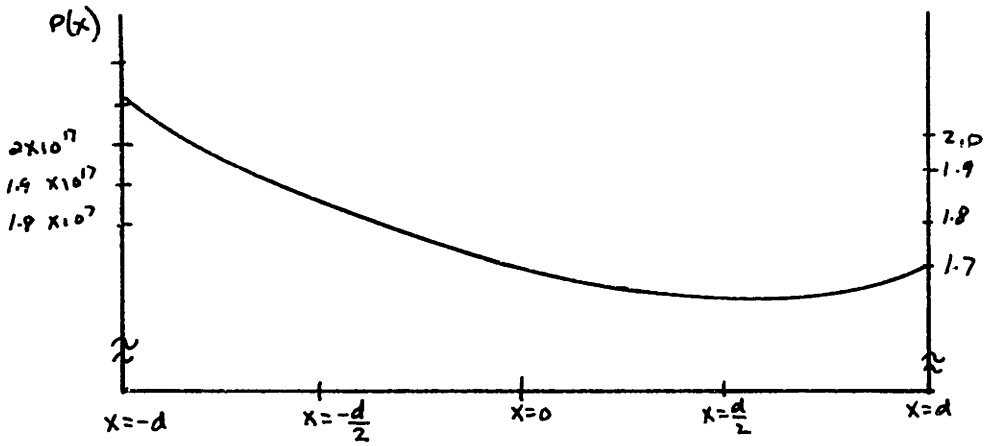

Figure 2.3

Since the minority carriers in the two highly dope regions can be neglected, Boltzmann equations at the boundaries become:

(2.12) $$p(-d) = p_0 e^{qV_p/kT}$$ V_p = VOLTAGE ACROSS P-I JUNCTION

(2.13) $$p(+d) = n_0 e^{qV_n/kT}$$ V_n = VOLTAGE ACROSS I-N JUNCTION

Combining (2.11), (2.12) and (2.13), we get:

(2.14) $$J = \frac{2qL_a n_i}{\tau} \frac{\tanh d/L_a}{\sqrt{1-B^2\tanh^4 d/L_a}} e^{q(V_p+V_n)/kT}$$

In calculating the voltage drop across the I region we must evaluate $\int_{-d}^{+d} E(x)dx$ where E is the electric field in the I region. Solving for the electric field we get under the high level injection condition:

(2.15) $$E(x) = \frac{J}{q(\mu_e+\mu_h)p} - \frac{kT}{q}\frac{B}{p}\frac{\partial p}{\partial x}$$

(2.16) $$V_I = +\int_{-d}^{d} E(x)\,dx = \frac{kT}{q}\left\{\frac{8b}{(b+1)^2}\frac{\sinh d/L_a}{\sqrt{1-B^2\tanh^4 d/L_a}}\tan^{-1}\left[\sqrt{1-B^2\tanh^4 d/L_a}\,\sinh d/L_a\right] + B\ln\frac{1+B\tanh^2 d/L_a}{1-B\tanh^2 d/L_a}\right\}$$

(2.17) $$\text{for } 2d/L_a \ll 1, \text{ then } V_I \simeq \frac{2kT}{q}\left(\frac{d}{L_a}\right)^2$$

Note that the total voltage drop across the diode is $V = V_I + V_p + V_n + V_{CONTACT}$

$V_{CONTACT} = I R_c$; R_c is the contact resistance and can be ignored.

Thus $V_p + V_n = V - V_I$ and substituting this into (2.14) we get:

$$J = J_S e^{q(V-V_I)/kT}$$

$$J_S = \frac{2qL_a n_i}{\tau}\frac{\tanh d/L_a}{\sqrt{1-B^2\tanh^4 d/L_a}}$$

Since the voltage is across the I region is approximately constant then:

(2.18) $$R_I \simeq \frac{2kT}{qI}\left(\frac{d}{L_a}\right)^2$$

Equation (2.18) can be put in a different form by using:

(2.19) $$L_a^2 = \frac{2bL_n^2}{b+1}, \text{ where } b = \frac{\mu_e}{\mu_n} \text{ and the EINSTEIN Relation } \frac{kT}{q} = \frac{D_n}{\mu_n}$$

Substituting these last two equations in (2.18) we get:

(2.20) $$R_I = \frac{W^2}{I\tau 2\bar{\mu}} \quad \text{where } W = 2d,\ \bar{\mu} = (\mu_e + \mu_n)/2$$

The method described in determining R_I is a rather complicated one. However, if we make the approximation that

$P(x) = C$ = constant in the I region, then the evaluation of is much simplified. Using the constitutive law:

(2.21) $$J = \sigma E$$

with $\sigma = \sigma(x) = q(n(x)\mu_e + p(x)\mu_p)$ and the charge neutrality condition $n(x) = p(x)$, we get:

$$\sigma(x) = p(x) q [\mu_e + \mu_n] = p(x) q 2\bar{\mu}$$

Substituting for (2.21) we get:

(2.22) $$E(x) = \frac{J}{q(\mu_e + \mu_n) p(x)}$$

Note that if we were to substitute the exact expression for $p(x)$ in (2.22), closed form evaluation of $\int E(x)dx$ would be impossible. If the approximation $p(x)$ = constant were made, then:

$$V_I = \int_{-d}^{d} E(x)dx = \frac{J(2d)}{q\, 2\bar{\mu}\, \bar{p}}$$

Multiplying numerator and denominator by $A(2d)$, we get:

$$V_I = \frac{JA(2d)^2}{q(\mu_e + \mu_n)\bar{p}\, A 2d} \qquad A = \text{cross sectional area}$$

But $[\bar{p} q A(2d)]$ is just the total stored charge. Thus:

$$V_I = \frac{I(2d)^2}{(\mu_e + \mu_n) Q}$$

But the total stored charge must obey $\frac{dQ}{dt} + \frac{Q}{\tau} = I$ and in the steady state $Q = I\tau$. Therefore:

$$V_I = \frac{(2d)^2}{(\mu_e + \mu_n)\tau} = \frac{W^2}{2\bar{\mu}\tau} \qquad W = 2d \qquad \bar{\mu} = \mu_e + \mu_n$$

And agrees with equation (2.20).

It is interesting that we choose as our value for

$$\bar{p} = \frac{1}{2d}\int_{-d}^{d} p(x)\,dx$$

$$= \frac{1}{2d}\int_{-d}^{+d} \frac{J L_a}{2kT \sinh 2d/L_a}\left[\frac{1}{\mu_e}\cosh\left(\frac{x+d}{L_a}\right) + \frac{1}{\mu_h}\cosh\left(\frac{x-d}{L}\right)\right]$$

$$= \frac{1}{2d}\,\frac{d\,J L_a^2}{kT \sinh 2d/L_a}\left[\frac{1}{\mu_e} L_a \sinh\frac{2d}{L_a} + \frac{1}{\mu_h} L_a \sinh\frac{2d}{L_a}\right]$$

$$\bar{p} = \frac{1}{2d}\,\frac{J L_a^2}{2kT}\left[\frac{1}{\mu_e} + \frac{1}{\mu_h}\right]$$

Now:

$$R_I = \frac{1}{\sigma}\frac{2d}{A}$$

$$= \frac{4d\,kT\,\mu_e\mu_h}{q J L_a^2 (\mu_e+\mu_h)}\left(\frac{2d}{A}\right)$$

Using $\frac{D_h}{\mu_h} = \frac{kT}{q}$ and $L_a^2 \approx D_h\tau$ and if $\mu_e \approx \mu_h$ then:

(2.23) $$R_I = \frac{(2d)^2}{I\tau(\mu_p+\mu_h)}$$

which is in close agreement with (2.20).

2.2 AC Analysis

The above analysis shows what happens at DC. When operating the diode at a high frequency, the mathematics becomes more difficult.

In doing an AC analysis we will consider the diode

current as $I = I_{DC} + I_{AC}\cos\omega t$. Consequently, the carrier concentration will be:

$$P(x,t) = P_{DC}(x) + P_{AC}(x,t)$$

$$p(x,t) = P_{DC}(x) + \text{Real}\left[F(x)e^{j\omega t}\right]$$

Because (2.7), the equation governing p(x,t), is a linear differential equation, we can superimpose the solution of the DC component with the AC component. Substituting the AC component in (2.7) we get:

$$\frac{d^2F}{dx^2} - \frac{F}{\lambda^2} = 0 \qquad \lambda = \frac{L_a}{\sqrt{1+j\omega\tau}}$$

The AC component must also satisfy the boundary conditions:

$$\left(\frac{\partial F}{\partial x}\right)\Big|_{x=-d} = \frac{-J_{ac}}{2\mu_h kT}$$

$$\left(\frac{\partial F}{\partial x}\right)\Big|_{x=d} = \frac{J_{ac}}{2\mu_e kT}$$

Solving for F(x), subject to the two boundary conditions, we get:

$$F(x) = \frac{J_{ac}\lambda\tau}{2q L_a^2}\left[\frac{\cosh x/\lambda}{\sinh d/\lambda} - B\frac{\sinh x/\lambda}{\cosh d/\lambda}\right], \text{ Now taking Real } \left[F(x)e^{j\omega t}\right],$$

(2.24)
$$P_{AC}(x,t) = \frac{J_{ac}\tau e^{-(d/L_a)\sqrt{\omega\tau/2}}}{q L_a\sqrt{\omega\tau}\;\pi}\left[\begin{array}{l}\mu_h e^{+(x/L_a)\sqrt{\omega\tau/2}}\cos\left[\frac{x-d}{L_a}\left(\frac{\omega\tau}{2}\right)+\omega t-\frac{\pi}{4}\right]+\\ \mu_e e^{-(x/L_a)\sqrt{\frac{\omega\tau}{2}}}\cos\left[\frac{-x+d}{L_a}\left(\frac{\omega\tau}{2}\right)+\omega t-\frac{\pi}{4}\right.\end{array}\right]$$

If $\mu_e \neq \mu_h$, this expression becomes identical to the one derived by Leenov. [11] Figure 2.4 is a plot of $P_{ac}(x,t)$.

$$I_{AC} = I_{DC} = 20 \text{ ma}$$

$$A = 10^{-4} \text{ cm}^2$$

$$L_a = 2.5 \times 10^{-3} \text{ cm}$$

$$\mu_e = 3\mu_h = 1350 \text{ cm}^2/\text{volt-sec}$$

$$\omega = 2\pi f = 2\pi \times 10^8 \text{ radians}$$

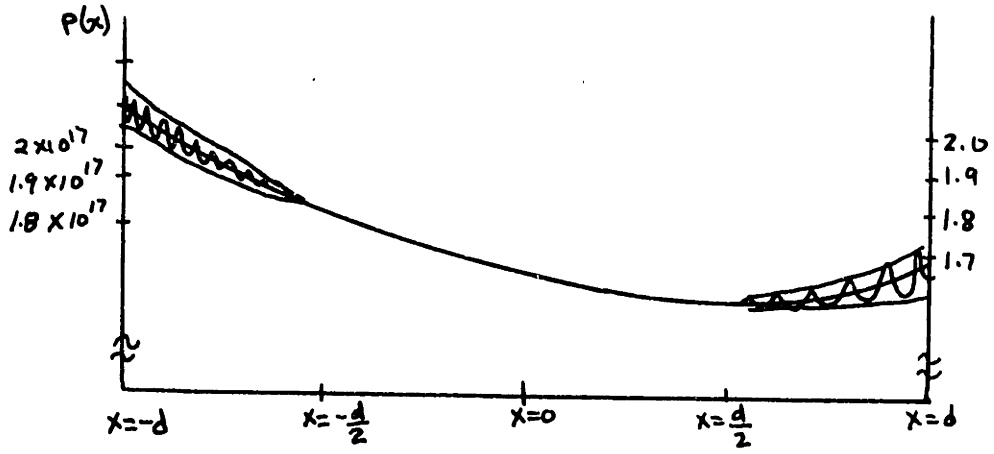

Figure 2.4

Thus far we have calculated an exact expression for $p(x,t)$. Because of the complexity of the function, $P_{ac}(x,t)$ like $P_{dc}(x)$ does not yield a close integral for:

$$\int_{-d}^{d} \frac{J}{q(\mu_e+\mu_h)p(x)}\,dx$$

Again, we must make the approximation that $p(x) = \bar{p}$ then we can write:

$$(2.25) \qquad R_I(t) = \frac{W^2}{2\bar{\mu}Q(t)}$$

where Q is the total stored charge in the I region. Using the continuity relation for Q and I:

$$(2.26) \qquad \frac{dQ}{dt} + \frac{Q}{\tau} = I$$

with $I = I_{dc} + I_{ac}\cos\omega t$, we get, solving for Q,

$$Q = I_{dc}\tau + \frac{I\tau}{\sqrt{1+\omega^2\tau^2}}\cos(\omega t+\varphi)$$

$$\varphi = -\tan^{-1}\omega\tau$$

$$R_I(t) = \frac{w^2}{2\bar{\mu}\left[I_{DC}\tau + \frac{I_{AC}\tau}{\sqrt{1+\omega^2\tau^2}}\cos(\omega t+\varphi)\right]}$$

$$R_I(t) = \frac{w^2}{2\bar{\mu} I_{DC}\tau\left[1 + \frac{I_{AC}/I_{DC}}{\sqrt{1+\omega^2\tau^2}}\cos[\omega t + \rho]\right]}$$

From equation (2.25) we can see that the resistance of a PIN diode is very nearly linear. We can, in fact, model the resistance as a charge controlled resistor:

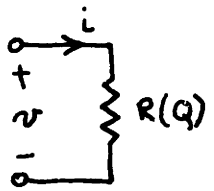

$$R(Q) = \frac{w^2}{2\bar{\mu} Q}$$

$$\frac{dQ}{dt} + \frac{Q}{\tau} = I$$

This equation, along with the charge continuity equation, $\frac{dQ}{dt} + \frac{Q}{\tau} = I$ is sufficient to describe the non-linear behavior of the diode.

2.3 Power Handling Capabilities

The presence of stored charge in the I region also increases the power capabilities of the diodes over ordinary P-N junction. Consider the simplified representation of a shunt switch:

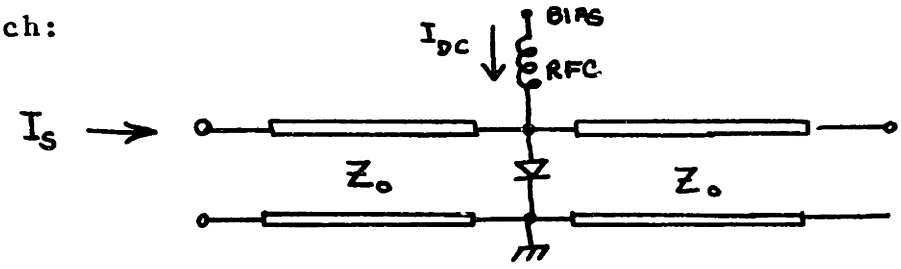

Figure 2.5

When the shunt is operating, that is, when the diode is forward biased, there will be stored charge, Q, in the I region:

$$Q = I_{dc}\tau_s$$

τ_s = carrier lifetime

I_{dc} = bias current

For positive cycles of the RF signal, the diode will obviously remain forward biased. On the negative half cycles, all the stored charge must be removed before the diode can change states. The amount of stored charge that must be removed is $I_{dc}\tau_s$.

For a sinusoidal RF signal, $Q = \frac{I_s}{j\omega_s}$ provided that This is the case with most PIN diode application. Equating the charge with the stored charge that must be removed, we can calculate the maximum RF signal level that can be switched.

$$I_{dc}\tau_s = \frac{I_s}{j\omega_s}$$

$$I_s = I_{dc}\tau_s j\omega_s$$

$$|I_s| = I_{DC}\tau_s\omega_s$$

For I_{dc} = 20 ma, $\tau_s = 2\pi$ x 100 Mhz, τ_s = 200 nanoseconds, I_s = 2.5 amperes. This corresponds to a power level of 130 watts. The other limitation on power level is that the duty cycle of the RF signal be sufficiently so that the junction temperature remains below its maximium rated temperature.

III Non-linearities

3.0 Introduction

In Section II, we have derived the I region resistance under DC conditions and under RF excitation. In the DC case:

$$R_I = \frac{w^2}{2\bar{\mu}\,\tau\, I_{DC}}$$

where w is the width of the I region and in the AC case:

$$R_I = R(t) = \frac{w^2}{2\bar{\mu}\, I_{DC}\,\tau\left[1+\frac{I_{AC}/I_{DC}}{\sqrt{1+\omega^2\tau^2}}(\cos\omega t+\varphi)\right]}$$

It is this non-linear time varying resistance that causes harmonic and intermodulation distortion.

There are two methods for calculating the non-linearities. One is to assume that the harmonics produced will not themselves produce any harmonics. Thus we can say that:

$$V(t) = R(t)I(t)$$

and by expanding R(t) in a Taylor series and using the various trigonometric identities, we can find the intermodulation products produced. This method is described in Section 3.1.

By assuming that V(t), Q(t), and I(t) are exponentials, and using

$$V(t) = V_0 + \frac{1}{2}\sum_{n=-\infty}^{\infty} V_n e^{j\omega_n t} \qquad \omega_n = n\omega$$

$$I(t) = I_0 + \frac{1}{2}\sum_{n=-\infty}^{\infty} I_n e^{j\omega_n t}$$

$$Q(t) = Q_0 + \frac{1}{2}\sum_{n=-\infty}^{\infty} Q_n e^{j\omega_n t}$$

and equation (2.25) and (2.26), and by matching coefficient of like frequencies, we can also get the resultant distortion. If simplifying assumptions are made, however, the results are identical to the linear resistance model described in Section 3.1. From ease of calculation viewpoint, the former is preferred.

3.1 Linear Resistance Method (Harmonic Distortion)

In calculating the non-linearities, we first assume that the system is nearly linear. Since the higher order harmonics do not contribute significantly to the low order products. We can then write: $V(t) = R(t)\, I(t)$

$$R(t) = \frac{w^2}{2\bar{\mu} I_{DC} \tau \left[1 + \frac{I_{AC}/I_{DC}}{\sqrt{1+w^2\tau^2}} (\cos \omega t + \varphi)\right]}$$

$$I(t) = I_{DC} + I_{AC} \cos \omega t$$

Assuming $\omega\tau \gg 1$, we get $\varphi = -\frac{\pi}{2}$ and $\cos(\omega t + \varphi) = \sin \omega t$

Therefore:

$$(3.1) \qquad V(t) = (I_{DC} + I_{AC} \cos \omega t) \frac{w^2}{2\bar{\mu} I_{DC} \tau \left[1 + \frac{I_{AC}/I_{DC}}{\sqrt{1+w^2\tau^2}} (\sin \omega t)\right]}$$

and expanding R(t) in a Taylor series with $\frac{I_{AC}/I_{DC}}{\sqrt{1+w^2\tau^2}} \gg 1$ we get:

$$V(t) = \frac{w^2}{2\bar{\mu} I_{DC} \tau} \left[I_{DC} + I_{AC} \cos \omega t - \frac{I_{AC}/I_{DC}}{\omega \tau} (I_{DC} + I_{AC} \cos \omega t) \sin \omega t + \right.$$

$$\left. \frac{(I_{AC}/I_{DC})^2}{\omega^2 \tau^2} (I_{DC} + I_{AC} \cos \omega t) (\sin \omega t)^2 - \ldots + \ldots \right]$$

Expanding the various trigonometric products and using the trigonometric identities:

$$\cos \varphi \sin \varphi = \frac{1}{2} \sin 2\varphi + \frac{1}{2}$$

$$\sin^2\varphi = \frac{1}{2} - \frac{1}{2}\cos 2\varphi$$

$$\cos^3\varphi = \frac{1}{4}\cos 3\varphi + \frac{3}{4}\cos\varphi$$

and collecting terms of like frequencies, we get:

$$V_o = \frac{w^2}{2\bar{\mu} I_{DC}\tau}\left[I_{DC} + \frac{\frac{1}{2}(I_{AC}/I_{DC})}{w\tau} I_{AC} + \cdots \text{higher order terms}\right]$$

$$V_o \approx \frac{w^2}{2\bar{\mu}\tau}$$

(3.2) at w $$v_1 = \frac{w^2}{2\bar{\mu}\tau I_{DC}}\left[I_{AC}\cos wt - \frac{(I_{AC}/I_{DC})}{w\tau} I_{DC}\sin wt + \frac{1}{2}\frac{(I_{AC}/I_{DC})^2}{w^2\tau^2} I_{AC}\cos wt - \cdots + \cdots\right]$$

$$v_1 \approx \frac{w^2}{2\bar{\mu}\tau}\left(\frac{I_{AC}}{I_{DC}}\right)\cos w t$$

(3.3) at $2w$ $$v_2 = \frac{w^2}{2\bar{\mu}\tau I_{DC}}\left[\frac{-1}{2}\frac{I_{AC}/I_{DC}}{w\tau} I_{AC}\sin 2wt + \frac{1}{2}\frac{(I_{AC}/I_{DC})^2}{(w\tau)^2} I_{DC}\cos 2wt - \cdots + \cdots\right]$$

$$v_2 \approx \frac{-w^2}{2\bar{\mu}\tau}\frac{1}{2}\left(\frac{I_{AC}}{I_{DC}}\right)^2\frac{1}{w\tau}\sin 2w_1 t$$

(3.4) at $3w$ $$v_3(t) \approx \frac{w^2}{2\bar{\mu}\tau}\left(-\frac{1}{4}\right)\left(\frac{I_{AC}}{I_{DC}}\right)^3\frac{1}{(w\tau)^2}\cos 3wt$$

3.2 Fourier Series Method (Harmonic Distortion)

Identical results can be arrived at by using a perturbation approach. [9], * The basic equations are the same:

---

* This method for calculating the distortion in PIN diode was first used by P. Chorney, Unitrode Corp., Watertown, Massachusetts.

(3.5) $$V = \frac{w^2 I}{2\bar{\mu} Q}$$

(3.6) $$\frac{dQ}{dt} + \frac{Q}{\tau} = I$$

(3.7) $$Q(t) = Q_{DC} + \frac{1}{2}\sum_{n=-\infty}^{\infty} Q_n e^{j\omega_n t} \qquad \omega_n = n\omega$$

(3.8) $$I(t) = I_{DC} + \frac{1}{2}\sum_{n=-\infty}^{\infty} I_n e^{j\omega_n t}$$

(3.9) $$V(t) = V_{DC} + \frac{1}{2}\sum_{n=-\infty}^{\infty} V_n e^{j\omega_n t}$$

Substituting (3.7) and (3.8) into (3.5), we get:

(3.10) $$I_n = (j\omega_n + \frac{1}{\tau}) Q_n \qquad \text{if } \omega\tau \gg 1 \text{, then}$$

$$I_n \approx j\omega_n Q_n \; ; \quad I_{DC} = Q_{DC}\tau$$

Rewriting (3.5), we get

$$VQ = \frac{w^2 I}{2\bar{\mu}\tau}$$

Substituting (3.7), (3.8), (3.9) and using the equations

$$\left.\begin{aligned} I_n^* &= I_{-n} \\ Q_n^* &= Q_{-n} \\ V_n^* &= V_{-n} \end{aligned}\right\} \text{ for real systems}$$

We get $V_{DC} = \frac{w^2}{2\bar{\mu}\tau}$ and at V_1

$$\left[\frac{V_{DC}Q_1}{2} + \frac{V_1 Q_{DC}}{2} + \frac{Q_2 V_1^*}{4} + \frac{V_2 Q_1^*}{4} + \frac{V_3 Q_2^*}{4} + \frac{V_2^* Q_3}{4} + \text{higher order terms}\right] e^{j\omega t} = \frac{w^2}{2\bar{\mu}} e^{j\omega t}$$

Note that $\frac{V_3 Q_2^*}{4}, \frac{V_2 Q_3^*}{4}, \frac{V_1^* Q_2}{4}, \frac{V_2 Q_1^*}{4} \ll \frac{V_{DC} Q_1}{2}$

and can be ignored. Thus we are left with:

$$\left[\frac{V_{0_1}Q_1}{2} + \frac{V_1 Q_{DC}}{2}\right] e^{j\omega t} = \frac{w^2}{2\bar{u}}\frac{I_1}{2} e^{j\omega t}$$

but $Q_1 = \frac{I_1}{j\omega}$ using (3.10)

$$\frac{V_{0_1}I_1}{2j\omega} + V_1 Q_{DC} = \frac{w^2 I_1}{2\bar{u}\ 2}$$

or $$V_1 = \frac{w^2}{2\bar{u}\,Q_{DC}} I_1 - \frac{V_0 I_1}{j\omega}$$

but $$\frac{w^2}{2\bar{u}\,Q_{DC}} >> \frac{w^2}{2\bar{u}\,Q_{DC}\,j\omega} = \frac{V_{0_1}}{j\omega}$$

(3.11) $$\therefore \quad V_1 = \frac{w^2}{2\bar{u}\,Q_{DC}} I_1$$

$$\sim \quad v_1 = \frac{1}{2}\left[V_1 e^{j\omega t} + V_1^* e^{-j\omega t}\right] = \frac{w^2}{2\bar{u}\,\tau}\left(\frac{I_{AC}}{I_{DC}}\right)\cos\omega t$$

This result is identical to (3.2). Solving for V_2 we get:

$$\left[\frac{V_{0_1}Q_2}{2} + \frac{V_2 Q_{DC}}{2} + \frac{V_1 Q_1}{4} + \frac{V_3 Q_1^*}{4} + \cdots\right] = \frac{1}{2}\frac{w^2}{2\bar{u}} I_2$$

Ignoring the last term and all higher order terms:

$$\frac{1}{2}\frac{w^2}{2\bar{u}} I_2 = \frac{V_{0_1}Q_2}{2} + \frac{V_2 Q_{DC}}{2} + \frac{V_1 Q_2}{4}$$

or

$$V_2 = \frac{w^2}{2\bar{u}\,Q_{DC}} I_2 - \frac{V_{0_1}Q_2}{Q_{DC}} - \frac{V_1 Q_1}{Q_{DC}\,2}$$

but $Q_2 = \frac{I_2}{j2\omega}$ and $Q_1 = \frac{I_1}{j\omega_1}$

$$V_2 = \frac{w^2}{2\bar{u}\,Q_{DC}} I_2 - \frac{V_{0_1}}{Q_{DC}}\frac{I_2}{-j2\omega_1} - \frac{V_1 I_1}{Q_{DC}\,j\,2\omega_1}$$

using $Q_{DC} = I_{DC}\tau$

$$V_2 = \frac{w^2}{2\bar{u}\,\tau}\frac{I_2}{I_{DC}} - \frac{V_{DC}}{I_{DC}}\frac{I_2}{-j2w\tau} - \frac{V_1 I_1}{2I_{DC}jw\tau}$$

$$= \frac{w^2}{2\bar{u}\,\tau I_{DC}}\left[1 - \frac{1}{2jw\tau}\right] - \frac{V_1 I_1}{2 I_{DC} jw\tau}$$

since $w\tau \gg 1$,

$$V_2 \approx \frac{w^2 I_2}{2\bar{u}\,\tau I_{DC}} - \frac{V_1 I_1}{2 I_{DC} jw\tau}$$

If the current through the diode has no significant component higher than I_1, then:

$$V_2 = \frac{-V_1 I_1}{2 I_{DC} jw\tau} \quad \text{or using (3.11)}$$

$$(3.12) \qquad V_2 = \frac{-w^2 I_1^2}{4\bar{u}\,\tau I_{DC}\, jw\tau}$$

$$U_2 = \frac{1}{2}\left[V_2 e^{jw_2 t} + V_2^* e^{jw_2 t}\right] = \frac{-w^2}{2\bar{u}\tau(w\tau)}\,\frac{1}{2}\left(\frac{I_{AC}}{I_{DC}}\right)^2 \cos 2wt$$

This is in agreement with equation (3.3). Similarly for the third harmonic we get:

$$\left[\frac{V_{DC} Q_3}{2} + \frac{Q_{DC} V_3}{2} + \frac{V_1 Q_2}{4} + \frac{V_2 Q_1}{4} + \cdots\right] = \frac{1}{2}\,\frac{w^2}{2\bar{u}\,\tau} I_3$$

Solving for V_3:

$$V_3 = \frac{w^2 I_3}{2\bar{u}\, Q_{DC}} - \frac{V_1 Q_2}{Q_{DC}\,2} - \frac{V_2 Q_1}{2\, Q_{DC}} - \frac{V_{DC}}{Q_{DC}}\,\frac{Q_3}{2}$$

using $Q_m = \frac{I_m}{jw_m}$

$$V_3 = \frac{w^2}{2\bar{\mu} Q_{DC}} I_3 - \frac{V_1 I_2}{I_{DC} j4w} - \frac{V_2 I_1}{2 I_{DC} \tau j w} - \frac{V_{DC} I_3}{Q_{DC} j w}$$

but $\frac{w^2}{2\bar{\mu} Q_{DC}} \gg \frac{V_{DC}}{Q_{DC} j 3w}$ and using (3.12)

$$V_3 = \frac{w^2}{2\bar{\mu} Q_{DC}} I_3 - \frac{V_1 I_2}{I_{DC} \tau j 4 w_1} - \frac{w^2}{2\bar{\mu} \tau I_{DC}} \frac{I_1^3}{I_{DC}^2 4 (w\tau)^2}$$

Again if the current has no harmonics, then $I_3 \approx 0$ and

$$v_3 = \frac{1}{2}\left(V_3 e^{j w_3 t} + V_3^* e^{-j w_3 t} \right),$$

or

$$v_3 = \frac{w^2}{2\bar{\mu} \tau (w\tau)^2} \left(\frac{-1}{4}\right) \left(\frac{I_{AC}}{I_{DC}}\right)^3 \cos 3wt$$

Again the results are identical with those derived by the linear resistance method.

It is obvious that although both methods will yeild identical results, given similar assumptions, the first is preferred.

3.3 Linear Resistance Method (Intermodulation Distortion)

In most applications, harmonic products can be filtered out. However, if there is intermodulation products, then in-band interference signals will result. (See Appendix A).

In analysing the intermodulation products, we will consider the PIN diode current to be approximately a two-tone signal, that is, a double sideband carrier surpressed signal.

Then $I = I_{dc} + I_{ac}[\cos w_1 t + \cos w_2 t]$. Because the equation relating I to Q, $\frac{dQ}{dt} + \frac{Q}{\tau} = I$ is linear, then the total stored charge will just be:

$$Q(t) = Q_{DC} + \frac{I_{ac}\tau}{\sqrt{1+\omega^2\tau^2}} \left[\cos(w_1 t + \varphi_1) + \cos(w_2 t + \varphi_2)\right] \quad \text{with } w_1 \neq w_2 \neq w$$

Thus, we can write:

$$R(t) = \frac{w^2}{2\bar{\mu}\tau I_{DC}} \frac{1}{\left[1 + \frac{I_{AC}/I_{DC}}{\sqrt{1+\omega^2\tau^2}}(\cos\omega_1 t + \varphi_1 + \cos\omega_2 t + \varphi_2)\right]}$$

$$\varphi_1 = -\tan^{-1}\omega_1\tau \qquad \varphi_2 = -\tan^{-1}\omega_2\tau$$

Expanding in a Taylor series and assuming $\omega\tau \gg 1$ so that $\cos\omega_1 t + \varphi_1 \approx \sin\omega_1 t$ and $\cos\omega_2 t + \varphi_2 \approx \sin\omega_2 t$ we get:

$$R(t) = \frac{w^2}{2\bar{\mu}\tau I_{DC}}\left[1 - \frac{I_{AC}/I_{DC}}{\omega\tau}(\sin\omega_1 t + \sin\omega_2 t) + \frac{\left(\frac{I_{AC}}{I_{DC}}\right)^2}{(\omega\tau)^2}(\sin\omega_1 t + \sin\omega_2 t)^2 - \frac{\left(\frac{I_{AC}}{I_{DC}}\right)^3}{(\omega\tau)^3}(\sin\omega_1 t + \sin\omega_2 t)^3 + \cdots\right]$$

With $V(t) = R(t)I(t)$.

Again, we must make use of trigonometric identities, and the Steinbrecher expansion for $[\cos\varphi_1 + \cos\varphi_2]^n$. [10] Expanding and collecting terms of like frequencies we get:

$$\text{at } \omega_1 \quad v_1 = \frac{w^2}{2\bar{\mu}\tau I_{DC}}\left\{I_{AC}\cos\omega_1 t + I_{DC}\left[-a\sin\omega_1 t - \tfrac{1}{4}a^3\sin\omega_1 t\right] + I_{AC}\left(a^2\sin\omega_1 t + \tfrac{1}{4}a^2\cos\omega_1 t\right)\right\} \qquad a = \frac{I_{DC}/I_{DC}}{\omega\tau}$$

$$\text{at } \omega_2 \quad v_2 = \frac{w^2}{2\bar{\mu}\tau I_{DC}}\left\{I_{AC}\cos\omega_2 t + I_{DC}\left[-a\sin\omega_2 t - \tfrac{1}{4}a^3\sin\omega_2 t\right] + I_{AC}\left(a^2\sin\omega_2 t + \tfrac{1}{4}a^2\cos\omega_2 t\right)\right\}$$

$$\text{at } 2\omega_1-\omega_2 \quad v=\frac{w^2}{2\bar{u}\tau I_{DC}}\left\{\begin{matrix} I_{DC}(-a^3)\frac{1}{2}\sin(2\omega_1-\omega_2)t + \\ I_{AC}\left[\left(-\frac{1}{4}\right)a^2\cos(2\omega_1-\omega_2)t + \frac{a^2}{2}\cos(2\omega_1-\omega_2)t\right]\end{matrix}\right\}$$

$$\text{at } 2\omega_2-\omega_1 \quad v=\frac{w^2}{2\bar{u}\tau I_{DC}}\left\{\begin{matrix} I_{DC}(-a^3)\frac{1}{2}\sin(2\omega_2-\omega_1)t + \\ I_{AC}\left[\left(-\frac{1}{4}\right)a^2\cos(2\omega_2-\omega_1)t + \frac{a^2}{2}\cos(2\omega_2-\omega_1)t\right]\end{matrix}\right\}$$

We have not collected terms for other frequencies because they are not inband signals and will not cause any significant interference with our signals. Note that for $w\tau \gg 1$ and $I_{AC}/I_{DC} < 1$

$$a=\frac{I_{AC}/I_{DC}}{\omega\tau} \ll 1$$

The greatest component at ω_1 and ω_2 is:

$$v_1=\frac{w^2}{2\bar{u}\tau I_{DC}} I_{AC}\cos\omega_1 t \qquad v_2=\frac{w^2}{2\bar{u}\tau I_{DC}} I_{AC}\cos\omega_2 t$$

Similarly, ignoring the other negligible terms at $2\omega_1-\omega_2$ and $2\omega_2-\omega_1$ we get:

$$v_{2\omega_1-\omega_2}=\left(\frac{-1}{4}\right)\frac{w^2}{2\bar{u}\tau(\omega\tau)^2}\left(\frac{I_{AC}}{I_{DC}}\right)^3\cos(2\omega_1-\omega_2)t$$

$$v_{2\omega_2-\omega_1}=\left(\frac{-1}{4}\right)\frac{w^2}{2\bar{u}\tau(\omega\tau)^2}\left(\frac{I_{AC}}{I_{DC}}\right)^3\cos(2\omega_2-\omega_1)t$$

3.4 Fourier Series Method (Intermodulation Product)

Again, identical results can be arrived at using a perturbation approach:

The basic equations are the same:

(3.13) $$VQ=\frac{w^2 I}{2\bar{u}}$$

$$\frac{dQ}{dt} + \frac{Q}{\tau} = I \tag{3.14}$$

But now, V(t), I(t), Q(t) contain intermodulation components:*

$$V(t) = V_{DC} + \frac{1}{2}\sum_m \sum_n V_{m,n}\, e^{j\left[\left(\frac{m+n}{2}\right)\omega_1 + \left(\frac{m-n}{2}\right)\omega_2\right]t} \tag{3.15}$$

$$Q(t) = Q_{DC} + \frac{1}{2}\sum_m \sum_n Q_{m,n}\, e^{j\left[\left(\frac{m+n}{2}\right)\omega_1 + \left(\frac{m-n}{2}\right)\omega_2\right]t} \tag{3.16}$$

$$I(t) = I_{DC} + \frac{1}{2}\sum_m \sum_n I_{m,n}\, e^{j\left[\left(\frac{m+n}{2}\right)\omega_1 + \left(\frac{m-n}{2}\right)\omega_2\right]t} \tag{3.17}$$

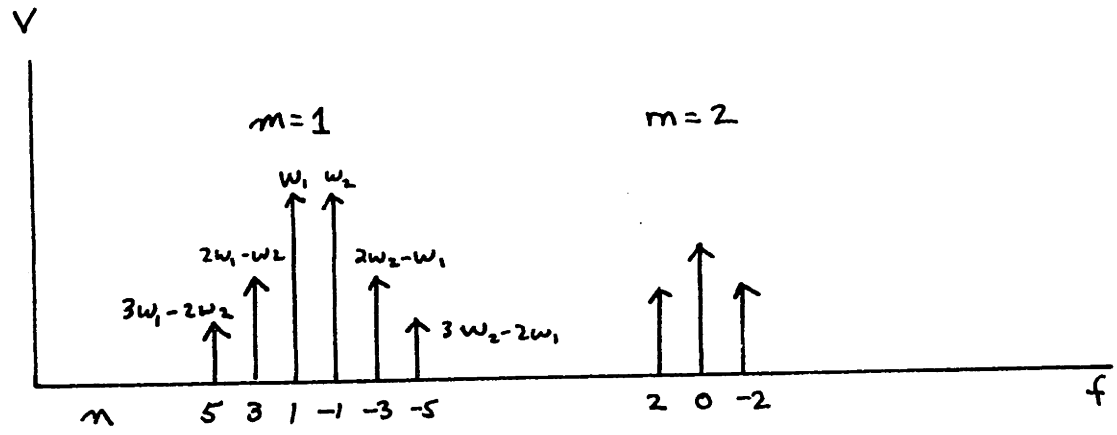

Figure 3.1 Intermodulation Product Spectrum

Using (3.14) and substituting in for I and Q, we have:

$$Q_{m,n} = \frac{I_{m,n}}{j\left(\frac{m+n}{2}\omega_1 + \frac{m-n}{2}\omega_2\right)}, \quad Q_{DC} = I_{DC}\tau \tag{3.18}$$

---

* See Appendix A for explanation of the notation used in denoting the frequencies.

Expanding (3.15):

$$V = V_0 + \frac{1}{2}\left(V_{1,1}e^{j\omega_1 t} + V_{1,1}^{*}e^{-j\omega_1 t}\right) + \frac{1}{2}\left(V_{1,-1}e^{j\omega_2 t} + V_{1,-1}^{*}e^{-j\omega_2 t}\right) +$$
$$\frac{1}{2}\left(V_{1,3}e^{j(2\omega_1-\omega_2)t} + V_{1,3}^{*}e^{-j(2\omega_1-\omega_2)t}\right) +$$
$$\frac{1}{2}\left(V_{1,-3}e^{j(2\omega_2-\omega_1)t} + V_{1,-3}^{*}e^{-j(2\omega_2-\omega_1)t}\right) + \cdots$$

Using the above expansion, and (3.13), then solving for $I_{1,-3}$ we have:

$$\frac{w^2}{2\bar{\mu}}\left(\frac{I_{1,-3}}{2}\right) = \frac{V_{DC}Q_{1,-3}}{2} + \frac{Q_{DC}V_{1,3}}{2} + \frac{V_{2,-2}Q_{1,1}^{*}}{4} + \frac{Q_{2,-2}V_{1,1}^{*}}{4} + \cdots$$

Simplifying and using (3.18), we get:

$$V_{1-3} = \left(\frac{w^2}{2\bar{\mu}\tau I_{DC}}\right)I_{1,-3} - \frac{V_{DC}}{I_{DC}\tau}\frac{I_{1,-3}}{j(2\omega_2-\omega_1)} + \frac{V_{2,-2}I_{1,2}^{*}}{2j\omega_1 I_0\tau} - \left(\frac{w^2}{2\bar{\mu}\tau I_{DC}}\right)\frac{I_{1,1}^{*}I_{2,-2}}{4j\omega_2 I_{DC}\tau}$$

but $\frac{V_0}{I_{DC}} = \frac{w^2}{2\bar{\mu}\tau I_{DC}}$ and $\frac{w^2}{2\bar{\mu}\tau I_{DC}} \gg \frac{w^2}{2\bar{\mu}\tau I_{DC}}\frac{1}{j(2\omega_2-\omega_1)\tau}$

$$\therefore V_{1-3} = \frac{w^2}{2\bar{\mu}\tau I_{DC}}I_{1,-3} + \frac{V_{2,-2}I_{1,1}^{*}}{j2\omega_1 I_{DC}\tau} - \left(\frac{w^2}{2\bar{\mu}\tau I_{DC}}\right)\frac{I_{1,1}^{*}I_{2,-2}}{4j\omega_2 I_{DC}\tau}$$

using $V = RI$, $V_{2,-2} = \left[\frac{w^2}{2\bar{\mu}\tau I_{DC}}\right]I_{2,-2}$ and

(3.12) $V_{2,-2} = \frac{-w^2}{2\bar{\mu}\tau I_{DC}}I_{1,-1}^{2}$

$$V_{1,-3} = \frac{w^2}{2\bar{\mu}\tau I_{DC}}I_{1,3} + \frac{V_{2,-2}I_{1,1}^{*}}{I_{DC}\tau}\left[\frac{1}{2j\omega_1} - \frac{1}{4j\omega_2}\right] \quad \text{for } \omega_1 \approx \omega_2$$

$$V_{1,-3} = \frac{w^2 I_{1,-3}}{2\bar{\mu}\tau I_{DC}} + \frac{1}{4}\frac{w^2 I_{1,1}^{*}I_{1,-1}^{2}}{2\bar{\mu}\tau I_{DC}\omega_1\omega_2(I_{DC}\tau)^2}$$

By choosing our time origin so $I = I_{DC} + I_{AC}\cos\omega t$

$$I_{1,1}^{*} = I_{1,-1} = I_{AC} \quad \text{and} \quad I_{1,-3} \approx 0$$

$$V_{1,-3} = \frac{-j}{4} \frac{W^2}{2\bar{\mu}\tau(\omega\tau)^2} \left(\frac{I_{AC}}{I_{DC}}\right)^3$$

Thus $v_{2\omega_2-\omega_1} = \frac{1}{2}\left(V_{1,-3}\, e^{j(2\omega_2-\omega_1)t} + V_{1,-3}^{*}\, e^{-j(2\omega_2-\omega_1)t}\right.$

or

$$v_{2\omega_2-\omega_1} = -\frac{1}{4} \frac{W^2}{2\bar{\mu}\tau(\omega\tau)^2} \left(\frac{I_{AC}}{I_{DC}}\right)^3 \cos 2\omega_2 - \omega_1 t$$

Again, this is in agreement with the results in Section 3.3.

Though both methods will yield identical results, the former is much simpler and in terms of ease of calculations more desirable.

IV Intermodulation Product Measurements

4.0 We have shown that the third order intermodulation product is:

$$(4.1) \qquad V_{1,-3} = -\frac{1}{4}\frac{W^2}{2\pi\tau(\omega\tau)^2}\left(\frac{I_{AC}}{I_{DC}}\right)^3 \cos(2\omega_2 - \omega_1)t$$

Qualitatively, their behavior agrees with actual measurements, that is, the third order intermodulation products decrease with increasing DC bias and increasing frequency.

In characterizing the intermodulation products quantitatively, we will use the intercept form as explained in Appendix A; the n^{th} order intermodulation product has a slope of n when plotted on a log P_{out} versus log P_{in} scale.

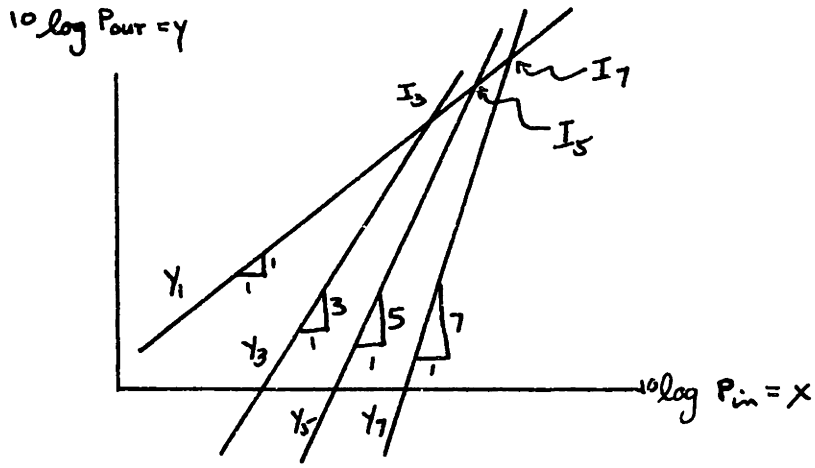

Figure 4.1 Intermodulation Products as a Function of Input Power Level

From Figure (4.1), we see that the fundamental component has a slope of 1:

$$(4.2) \qquad y_1 = x_1 \qquad y_1 = 10\log(P_{out,\,1}) \qquad x_1 = 10\log(P_{in,\,1})$$

The n^{th} order intermodulation products must go as:

$$(4.3) \qquad y_n = nx_n + b_n \qquad y_n = 10\log P_{out,\,n} \qquad b_n = \text{constant}$$

Now at the n^{th} order intercept, $y_n = y_1$, therefore $x_1 = nx_1 + b_n$

or $x_1 = \frac{-b}{n-1}$

Solving for b_n from (4.3), we have:

$$b_n = \frac{nx_1 - y_n}{n-1} = x_1 + \frac{x_1 - x_n}{n-1}$$

$$\therefore \quad I_n = 10 \log P_{in,1} + \frac{10(\log P_{out,1} - \log P_{out,n})}{n-1}$$

For the third order intercept, we have:

$$I_3 = 10 \log P_{in,1} + \frac{10[\log P_{out,1} - \log P_{out,3}]}{2} \tag{4.4}$$

The characteristic that makes PIN diodes desirable for microwave applications also makes their characterization difficult, i.e., their very low distortion levels. It is not uncommon to find the harmonic content of the PIN diodes to be 50 - 120 db below the fundamental. This far exceeds the dynamic range of any available spectrum analyzer.

Using a cancellation scheme developed by D.H. Steinbrecher and R. Mohlere, it is possible to observe these low level signals adjacent to signals 50 - 120 db stronger. Figure 4.2 is a diagram of the cancellation device.

The two-tone signals are fed in and amplified by 12 db and attenuated by 12 db. (This isolates the oscillators from the rest of the cancellation device.) The two-tone signal is then divided by a hybrid. The signals in arms 1 and 3 are then adjusted with respect to phase and amplitude in order to cancel the two primary signals at the output.

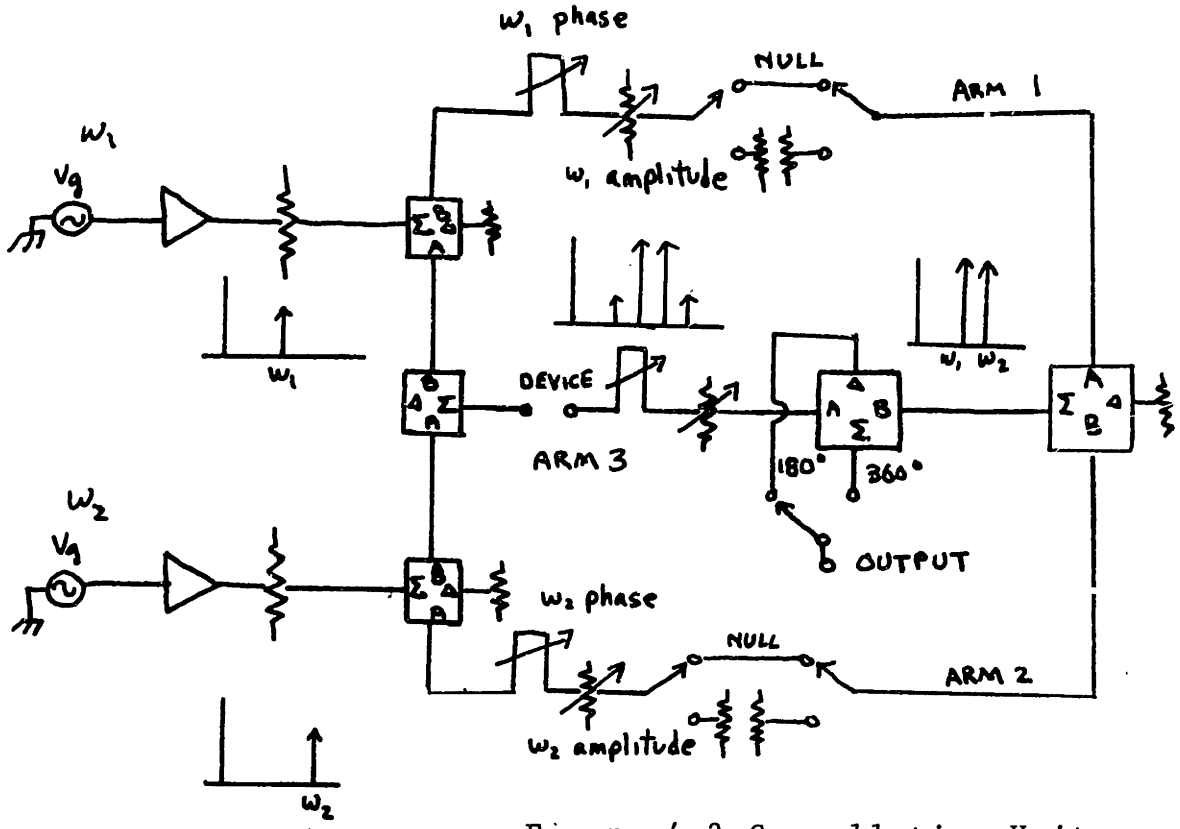

Figure 4.2 Cancellation Unit

Attached to the cancellation unit is a special PIN diode mounting. (Figure 4.3).

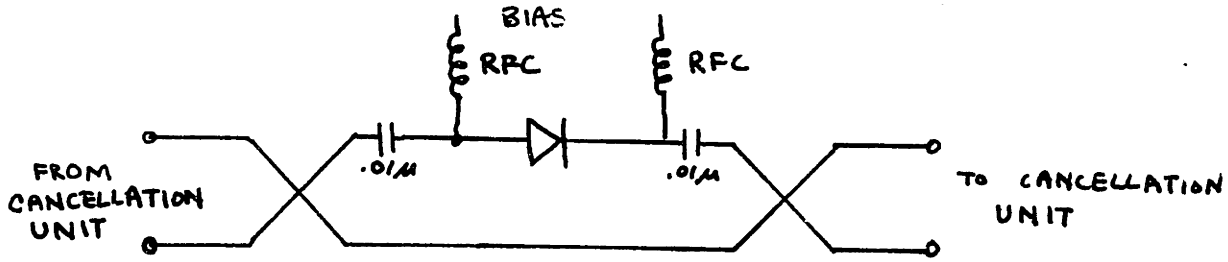

Figure 4.3 PIN Diode Mount

The equivalent circuit of the PIN diode and the cancellation unit is given in Figure 4.4.

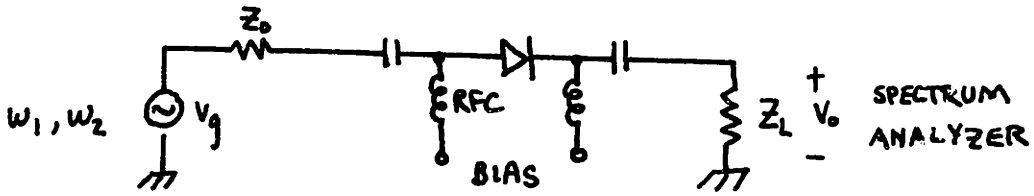

Figure 4.4 Equivalent Circuit

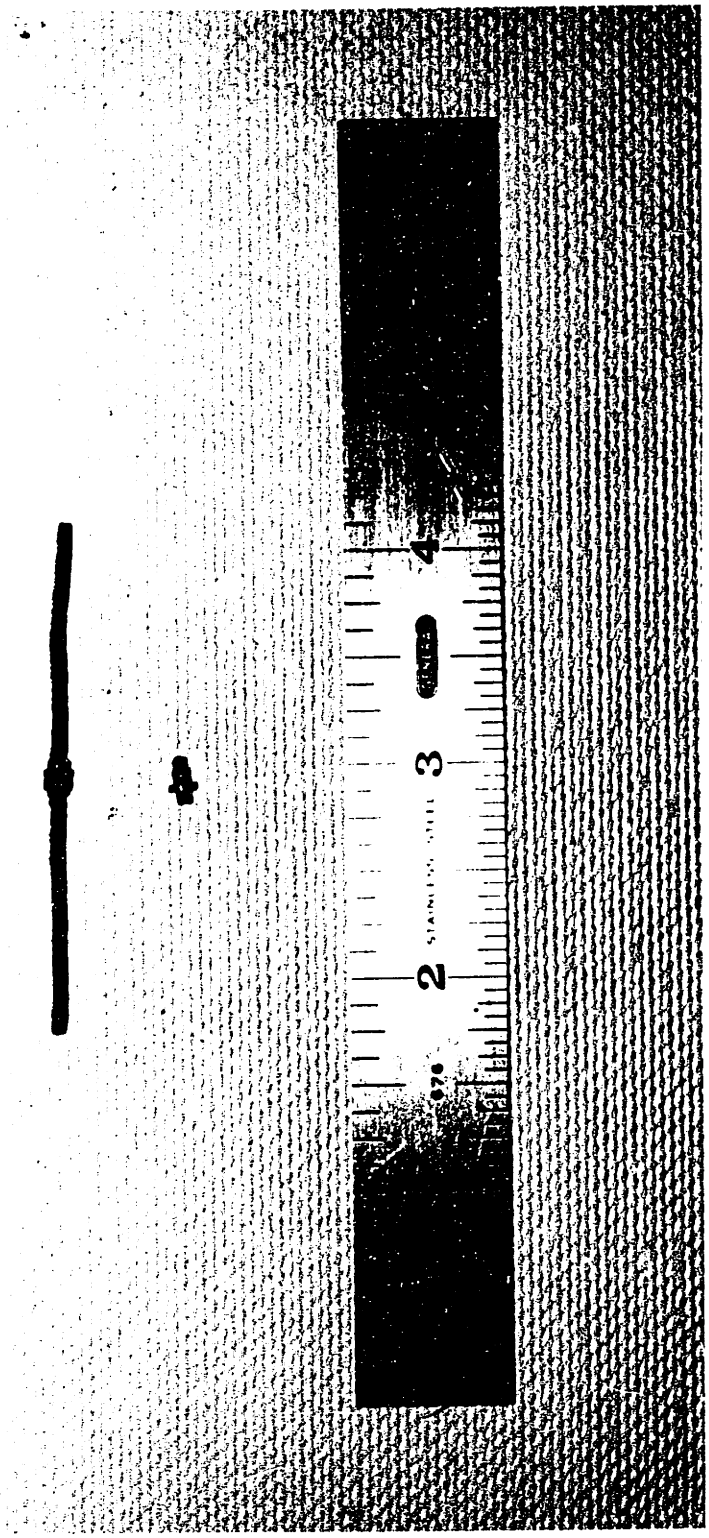

Figure 4.5 2 PIN diodes

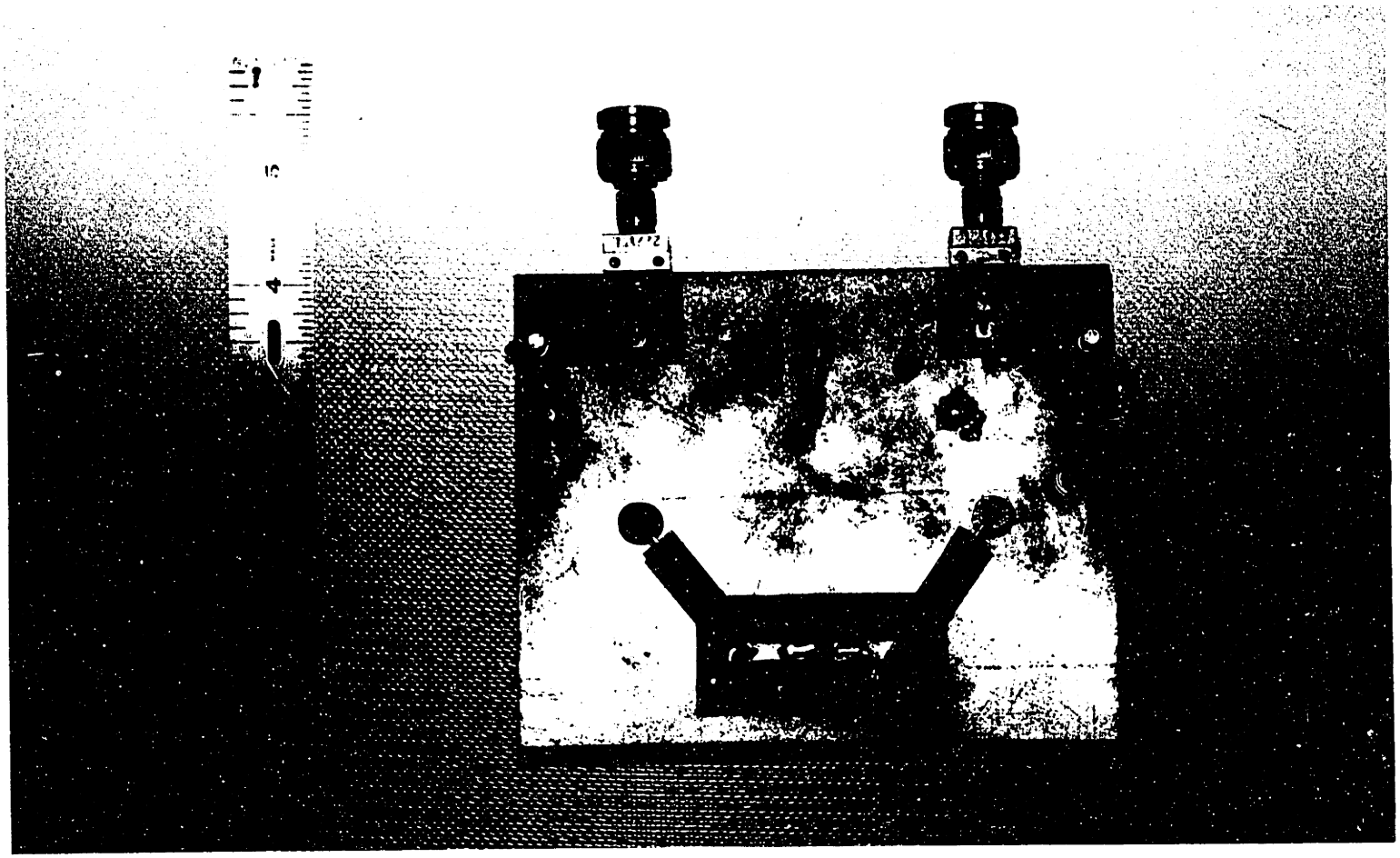

Figure 4.6 PIN Diode Mounting Circuit Side 1

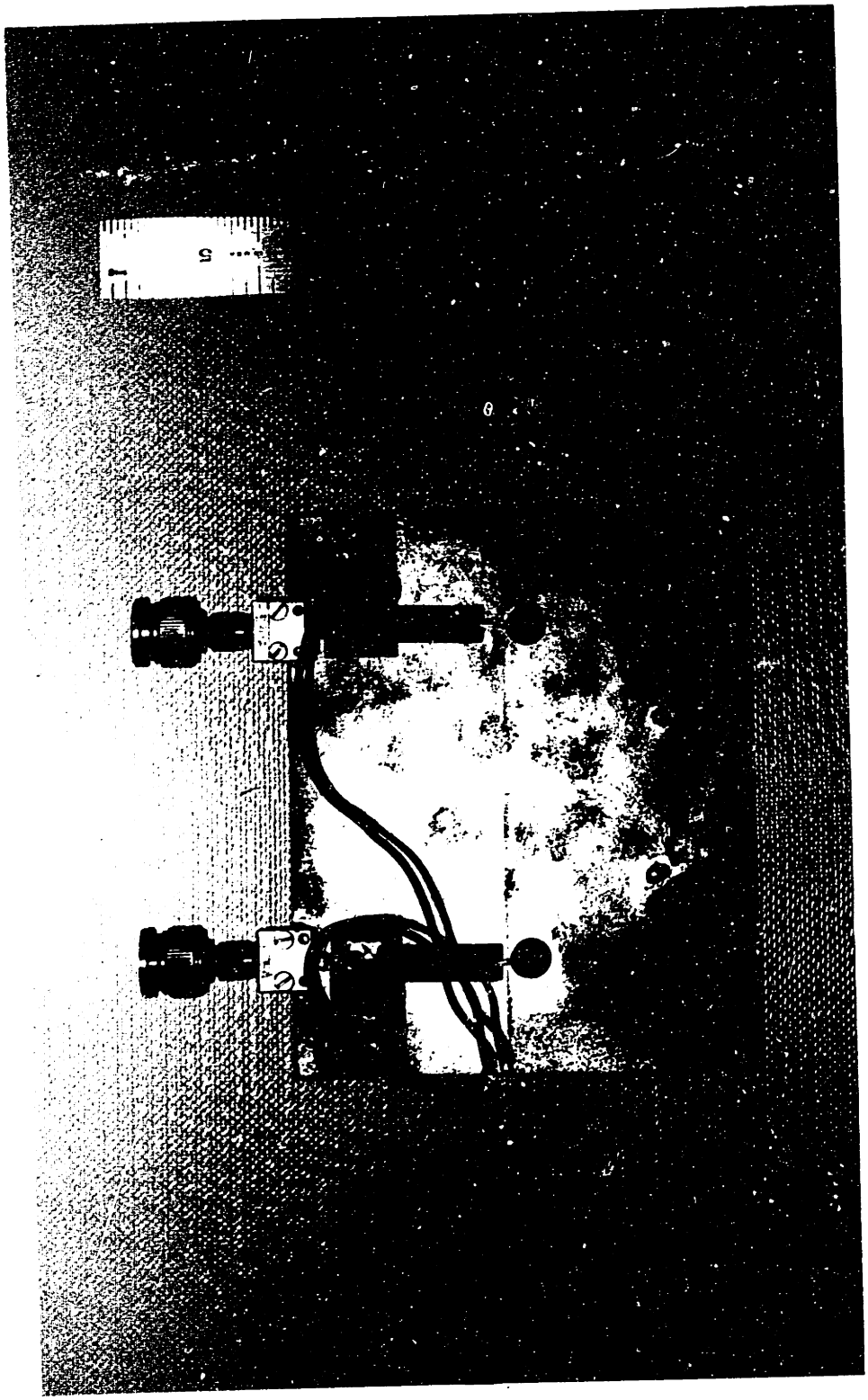

Figure 4.7 PIN Diode Mounting Circuit Side 2

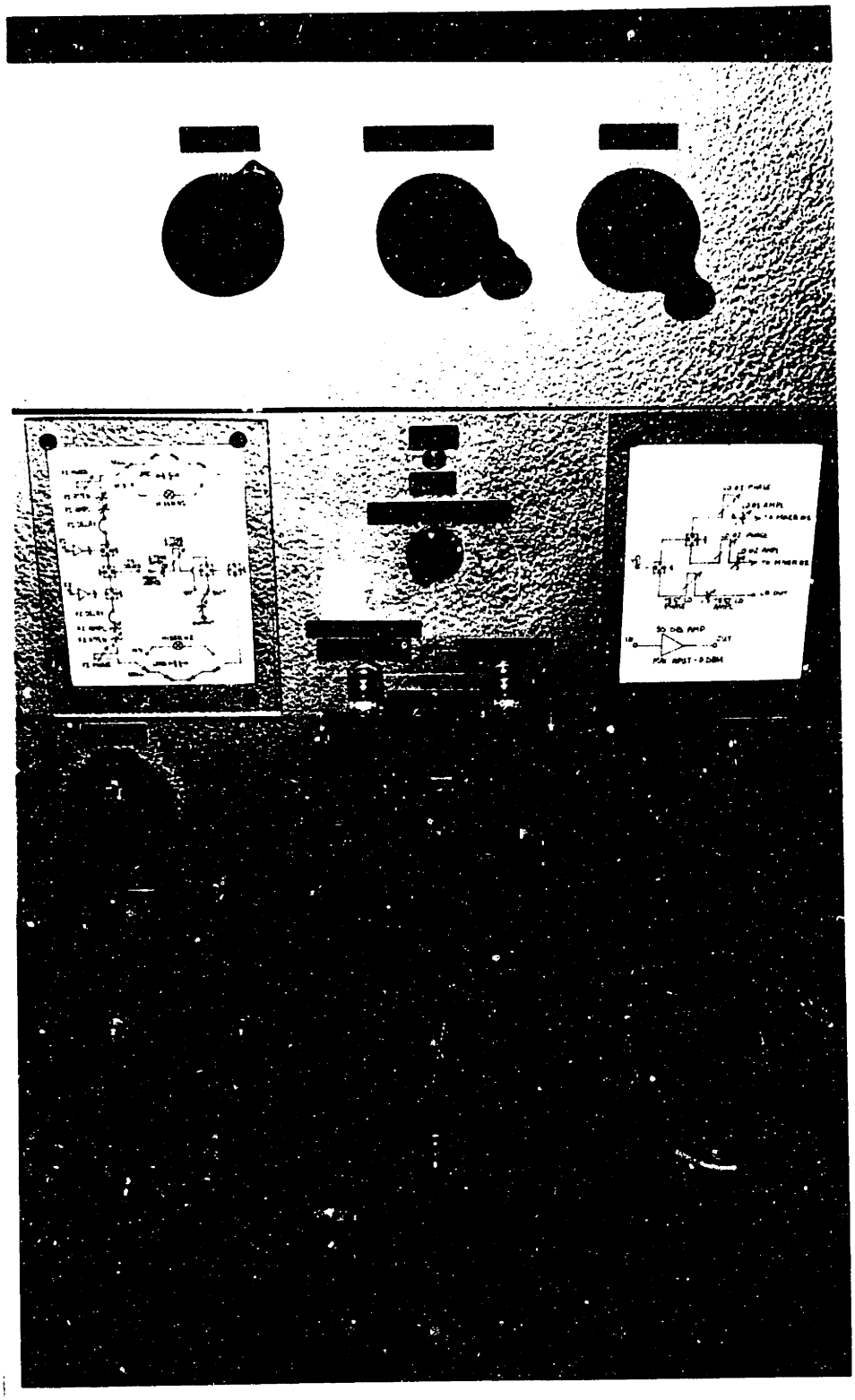

Figure 4.8 Cancellation Unit

In this circuit at ω_1 or ω_2 when the diode is forward biased

$$V_0 \cong \frac{Z_L}{2Z_0} V_g \approx \frac{1}{2} V_g \qquad Z_0 = Z_L$$

Therefore, the time average power is:

$$\frac{1}{2Z_0}\left(\frac{V_g}{2}\right)^2 = \frac{1}{8}\frac{V_g^2}{Z_0}$$

At the upper third order product the equivalent circuit is shown in Figure 4.9

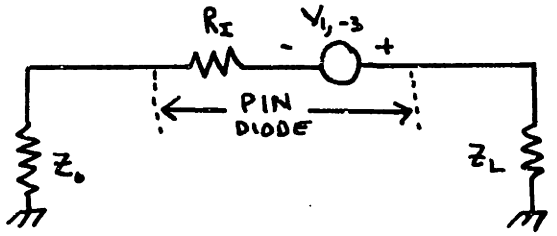

Figure 4.9

and

$$V_0\Big|_{2\omega_2-\omega_1} \cong \frac{Z_0}{2Z_0} V_{1,-3} = \frac{1}{2} V_{1,-3}$$

and time average power is:

$$(4.5) \qquad \frac{1}{8}\frac{V_3^2}{Z_0} = \frac{1}{8Z_0}\left[\frac{1}{4}\frac{W^2}{2\pi\tau(\omega\tau)^3}\left(\frac{I_{ac}}{I_{DC}}\right)^3\right]^2$$

4.1 Theoretical Calculations of Third-Order Intercepts

In calculating the theoretical intercept, we will assume that Z_0 = 50 ohms, and that the forward impedance of the diode is about 0.5 ohms. Using a reference power level of 1 dbm:

$$I_3 = \frac{-10 \log P_{OUT,3}}{2}$$

where $P_{out,3}$ is the 3rd order intermodulation product power level.

Using the network shown in Figure 4.4; $I_{ac} = \frac{V_L}{Z_0}$ at 1 dbm with Z_0 = 50 ohms: $\frac{V_L^2}{2Z_0} = 10^{-3}$ or $V_L^2 = 10^{-4}$ VOLTS^2

Substituting the last tow equations into (4.5) along with

$\bar{\mu}$ = .2 m^2/volt-sec
τ = 210 nanoseconds
W = 13 microns
} for Varian diodes

we get: $P_3 = \frac{1.78 \times 10^{12}}{\tau^6 f^4 I_{DC}^6}$

τ = carrier lifetime in nanoseconds

f = frequency in Mhz

I = current in milliamperes

In terms of dbm we get:

(4.6) $P^I = 10\log P_3/10^{-3}$

$= 152.3 - 60\log - 40 \log f - 60\log I_{dc}$

The third order intermodulation product level written in intercept form using equation (4.6) becomes $I_3 = 10\log P^I$

(4.7) $I_3 = -76 + 30\log + 40\log f + 30\log I_{dc}$

4.2 Measured Results

Measurements on third order intermodulation products were made at various frequencies and bias levels on four PIN diodes.

	Diode number	Carrier lifetime
Varian	VSD211N20-1	215 nanoseconds
Varian	VSD211N20-2	220 nanoseconds
Varian	VSD211N20-4	185 nanoseconds
Unitrode	UM4001B	5000 nanoseconds

The third order intercept for the Varian diodes along with the theoretical intercepts are plotted as a function of frequency and current. No plots were moade for the Unitrode UM4001B diode because no intermodulation products were observed. From equation (4.6) we see that the third order intermodulation product decreases 60 db per decade increase in carrier lifetime. Thus, with a carrier lifetime of 5 microseconds, 25 times as long as the Varian diodes, we can expect the third order intermodulation products to be at least 160 db below the primary signals. These levels are beyond that of the cancellation unit.

The frequencies used were:

f_1	f_2	
10.00	10.05	Mhz
12.00	12.05	Mhz
15.00	15.05	Mhz
20.00	20.05	Mhz
30.00	30.05	Mhz
40.00	40.05	Mhz

The bias levels used were 6, 10, 12, 15, 20, 30 milliamperes.

All graphs in this report contain two plots, one a theoretical intercept versus either bias current or frequency, the other a measured third order intercept.

Figures4.10, 4.11, 4.12 are plots of I_3 versus frequency at bias levels of 6, 10, and 15 milliamperes respectively for the Varian PIN diode VSD211N20-1. As shown, the theoretical and measured intercepts differ by no more than four db.

This is within the accuracy of the methods used. Possible errors can result from measurement of physical parameters of the diodes, measuring the intermodulation levels on the spectrum analyzer, input power errors and, of course, the approximation used for the carrier profile.

Figure 4.13 and Figure 4.14 are a plot of I_3 versus I_{dc} at frequencies of 10.00, 10.05 Mhz and 15.00, 15.05 Mhz respectively. There is a significant error between the theoretical and measured slopes.

In calculating the third-order intercept we assumed that the carrier lifetime and the width of the I region remained independent of bias current. Consequently the predicted third order intercept has a 30 db/decade current dope. However, carrier lifetime decreases with increased current and I region width increases with increasing bias current. Their effects are to decrease the slope of I_3 versus I_{dc}. To the best of the author's knowledge, little or no theoretical work has been done in determining the exact relation between I region width and current; and carrier lifetime and current. Some empirical relations have been determined. [11] Figures 4.15, 4.16, 4.17, 4.18 and 4.19 are intercepts versus frequency and current for the Varian VSD211N20-2 PIN diode. Again, there is a significant error in Figures 4.18 and 4.19, the intercept plotte as a function of current.

Figures 4.20, 4.21, 4.22, 4.23 and 4.24 are intercept versus frequency and current for the Varian VSD211N20-4 PIN diode. There are errors in all slopes, the greatest in Figures 4.23 and 4.24. One possible explanation is that this diode was

the first one used in making intermodulation measurements and thus subjected to more shock, more junction heating and other conditions that may affect the device parameters. This is in addition to the other sources of errors discussed previously.

Other than the last diode, all of the PIN diode intercepts were within 10 db of the theoretical intercepts in the frequency range of 10 - 40 Mhz and in the current range of 6 - 30 milli-amperes.

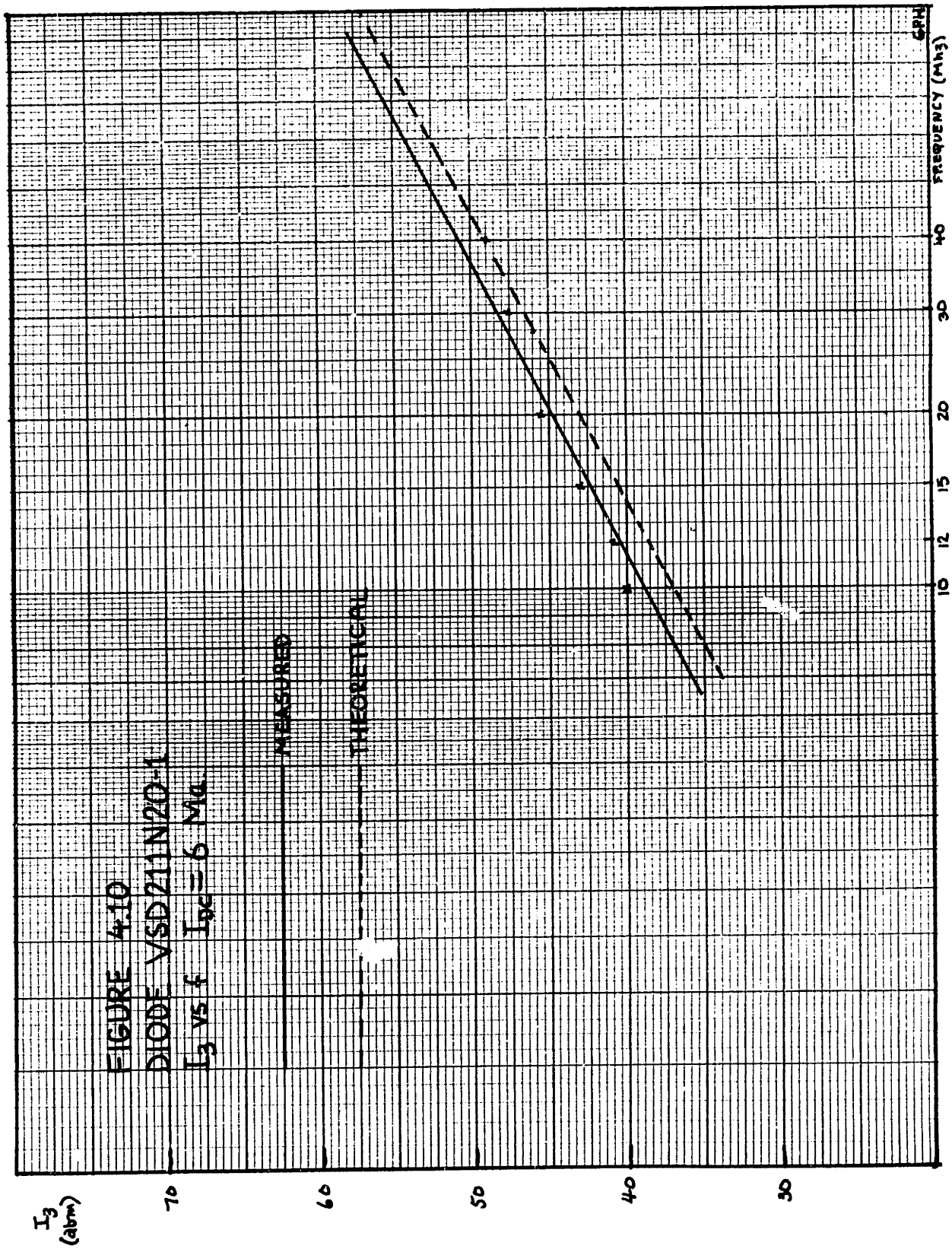
FIGURE 4.10
DIODE VSD211N20-1
I_3 vs f I_{DC}=6 MA
MEASURED
THEORETICAL
I_3 (dbm)
70
60
50
40
30
10
12
15
20
30
40
GPH
FREQUENCY (MHz)

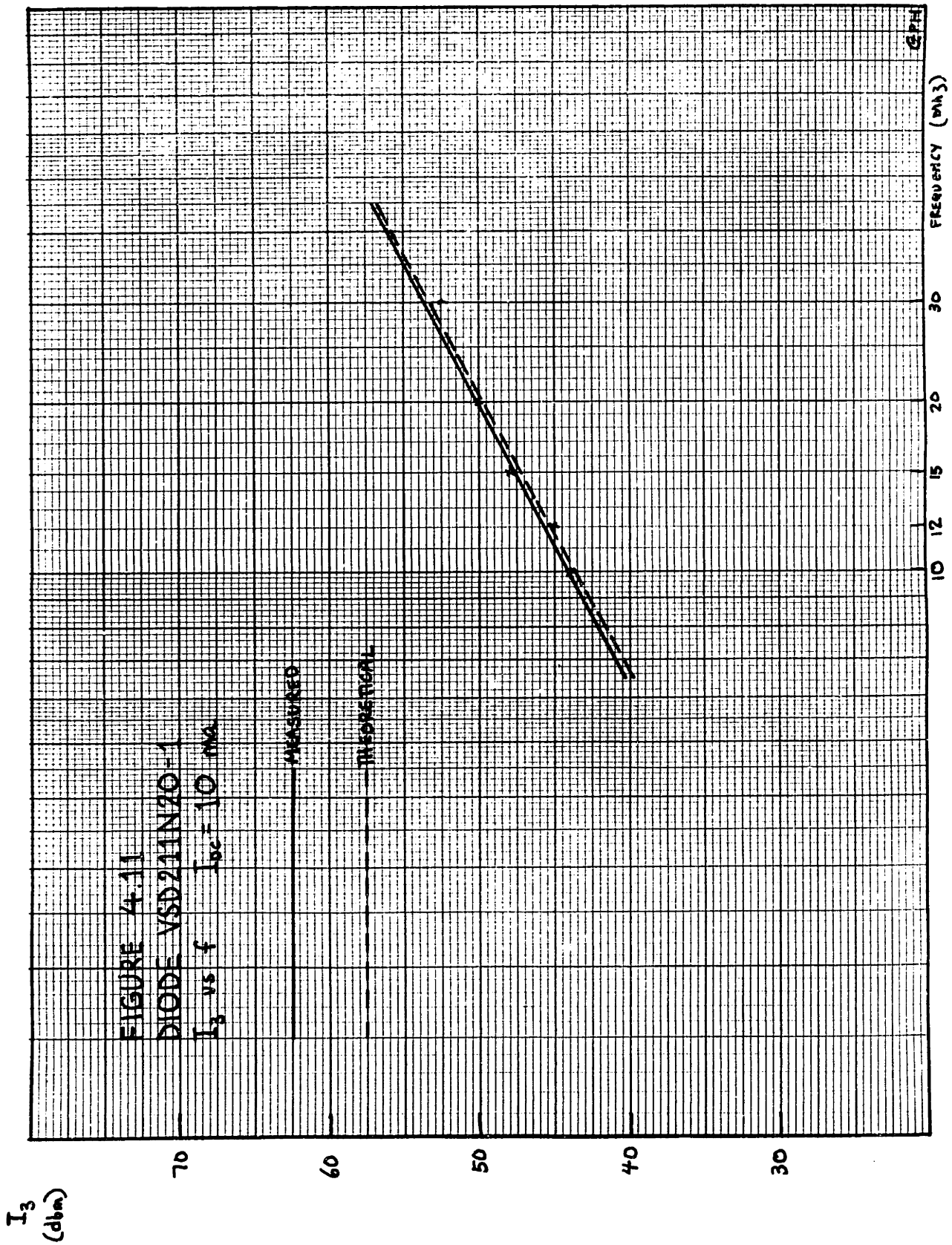
FIGURE 4.11
DIODE VSD211N20-1
I_3 vs f I_{DC}=10 mA
MEASURED
THEORETICAL
I_3 (dBm)
70
60
50
40
30
10
12
15
20
30
FREQUENCY (MHz)
GPH

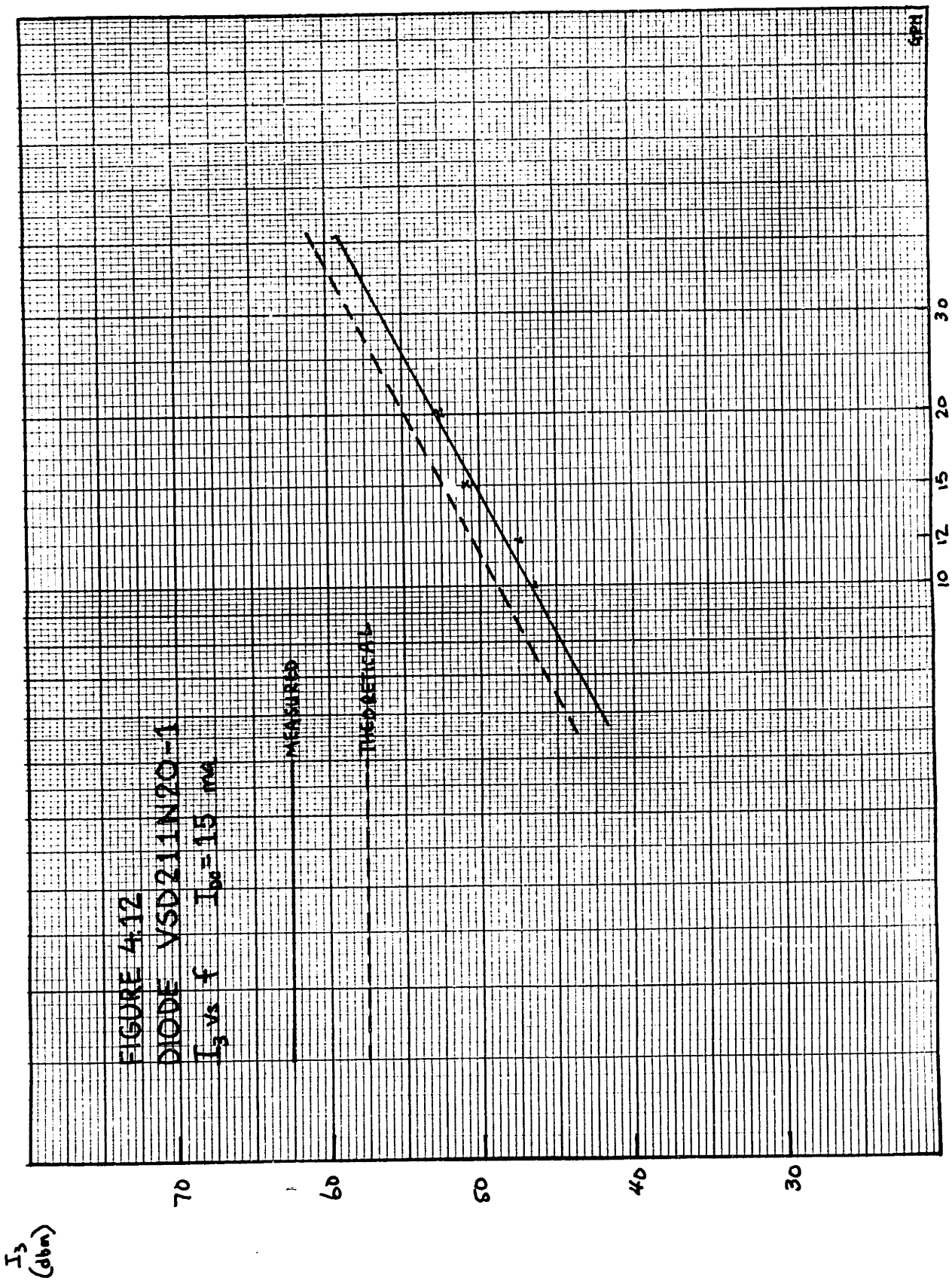
FIGURE 4.12
DIODE VSD211N20-1
I_S vs f I_{DS}=15 mA
MEASURED
THEORETICAL
I_S (pA)
70
60
50
40
30
10
12
15
20
30
MHz

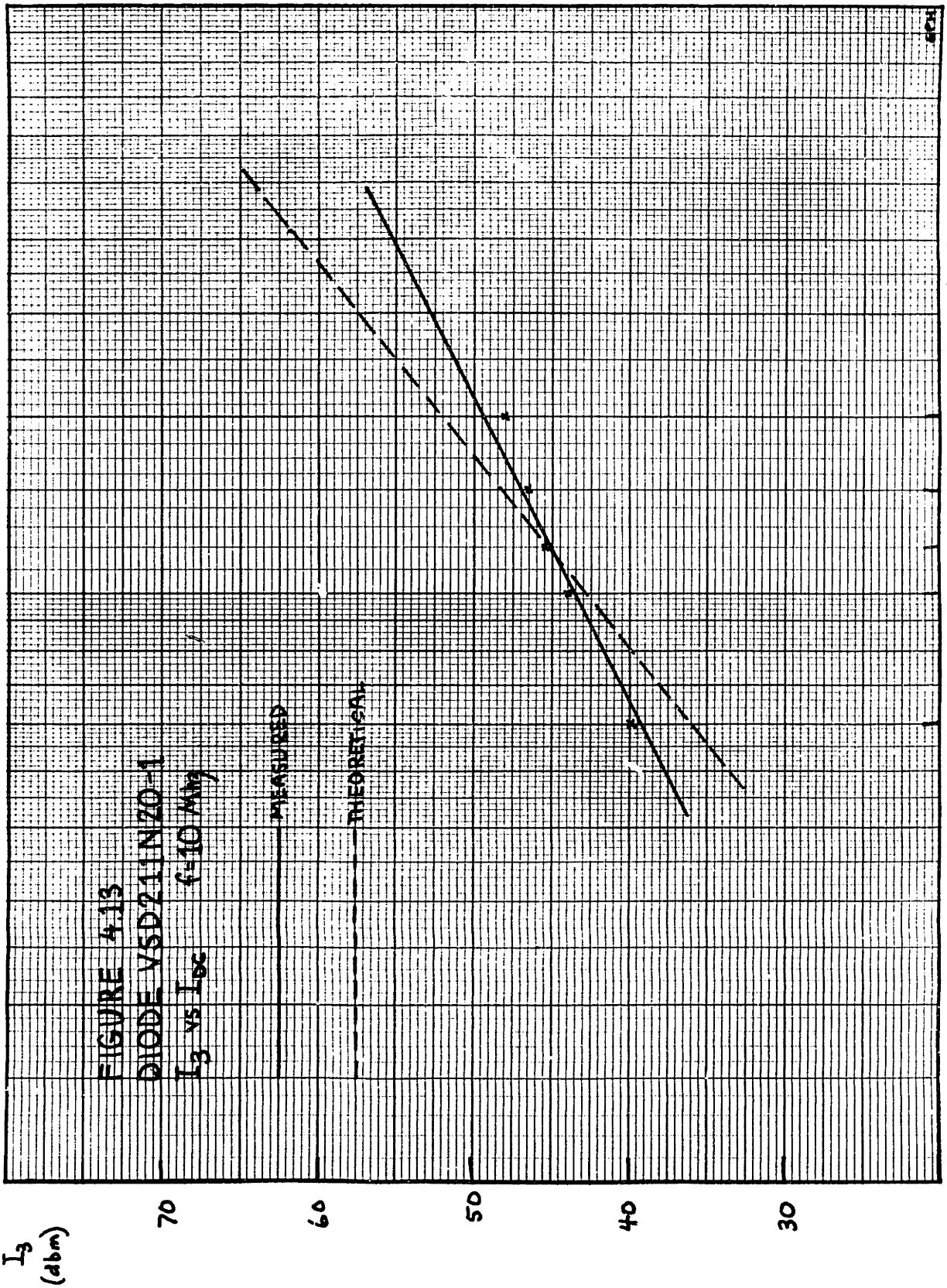
FIGURE 4.13
DIODE VSD2.1N20-1
I_3 vs I_{sc} f=10 Mhz
MEASURED
THEORETICAL
I_3 (dbm)
70
60
50
40
30
6
10
12
15
20
I_{sc} (ma)

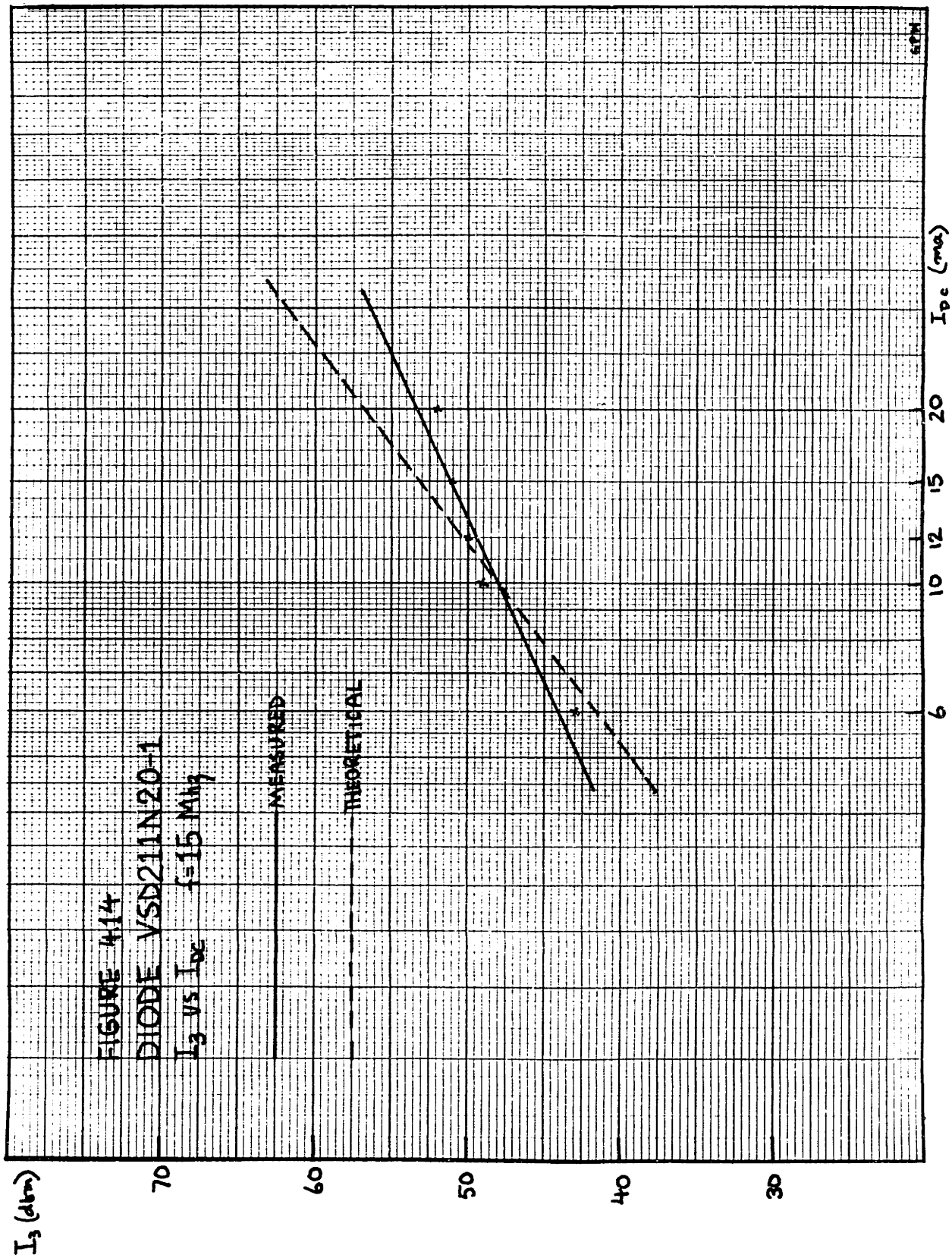
FIGURE 4.14
DIODE VSD211N20-1
I_3 vs I_{DC} f=15 MHz
MEASURED
THEORETICAL
I_3 (dbm)
70
60
50
40
30
6
10
12
15
20
I_{DC} (ma)

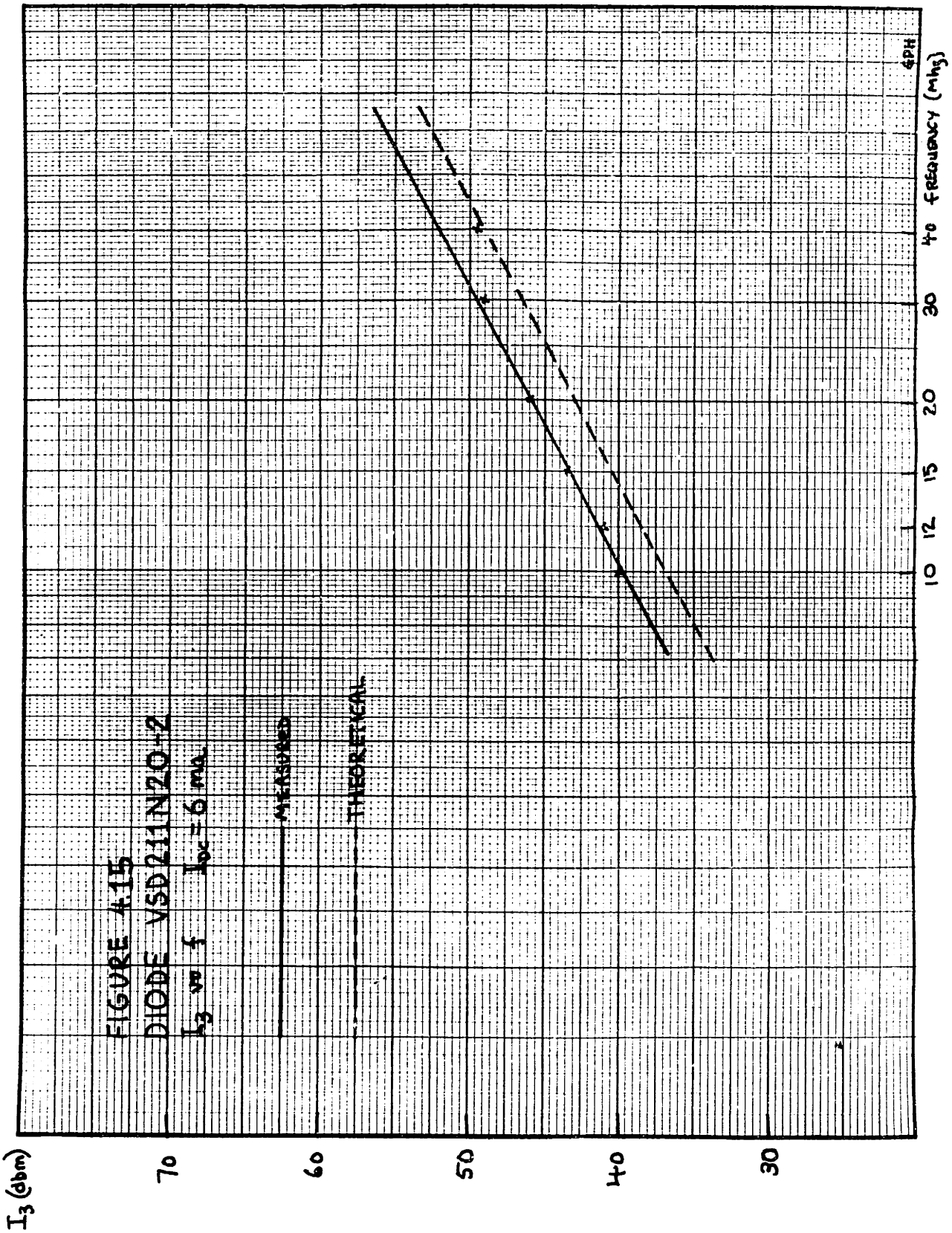
FIGURE 4.15
DIODE VSD211N20-2
I_3 vs f I_{DC} = 6 ma.
MEASURED
THEORETICAL
I_3 (dbm)
70
60
50
40
30
10 12 15 20 30 40 FREQUENCY (mhz)
4PH

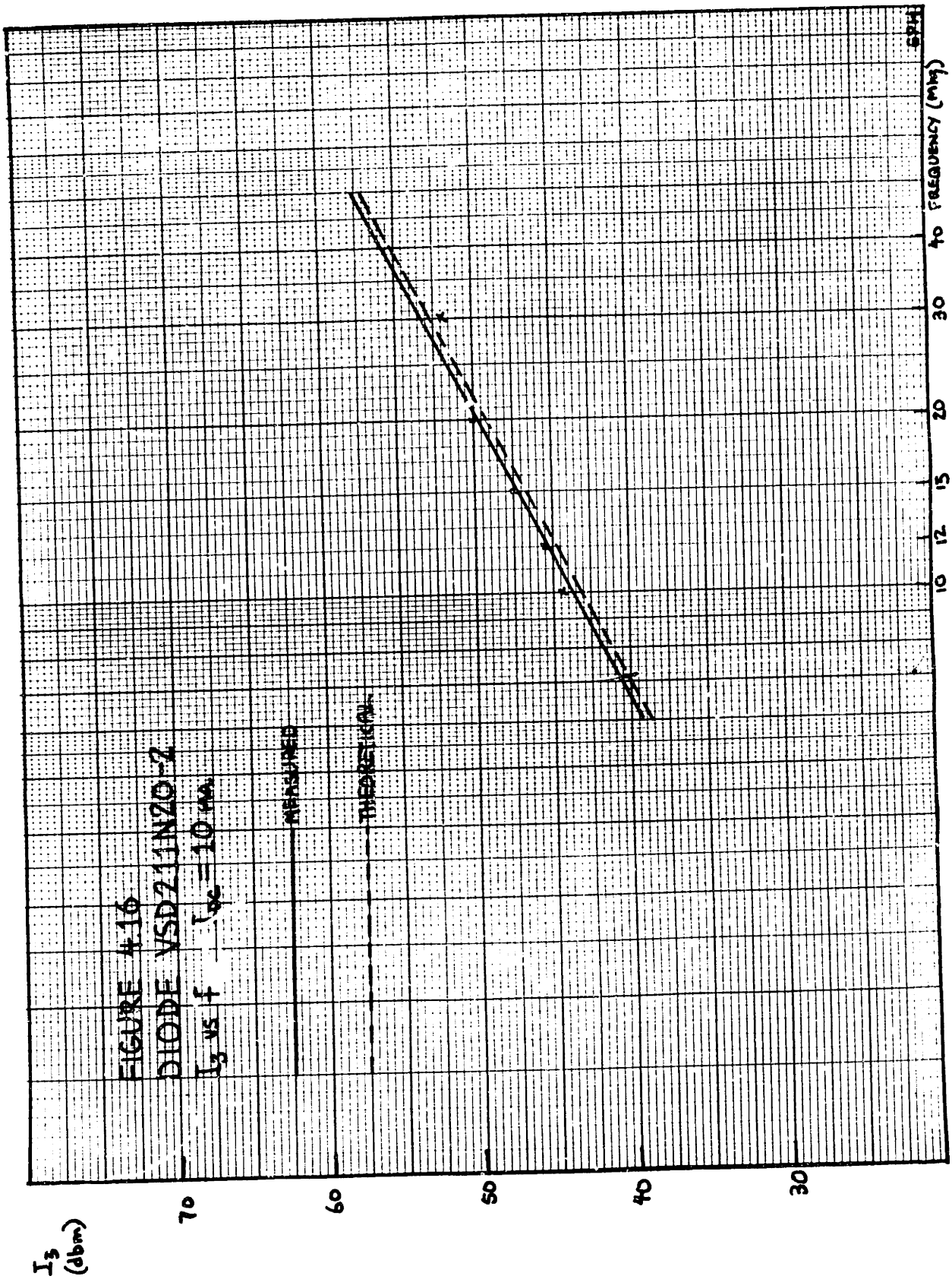
FIGURE 4.16
DIODE VSD211N20-2
I_s vs f — I_{DC} = 10 mA
MEASURED
THEORETICAL
I_s (dbm)
70
60
50
40
30
10
12
15
20
30
40
GHz
FREQUENCY (MHz)

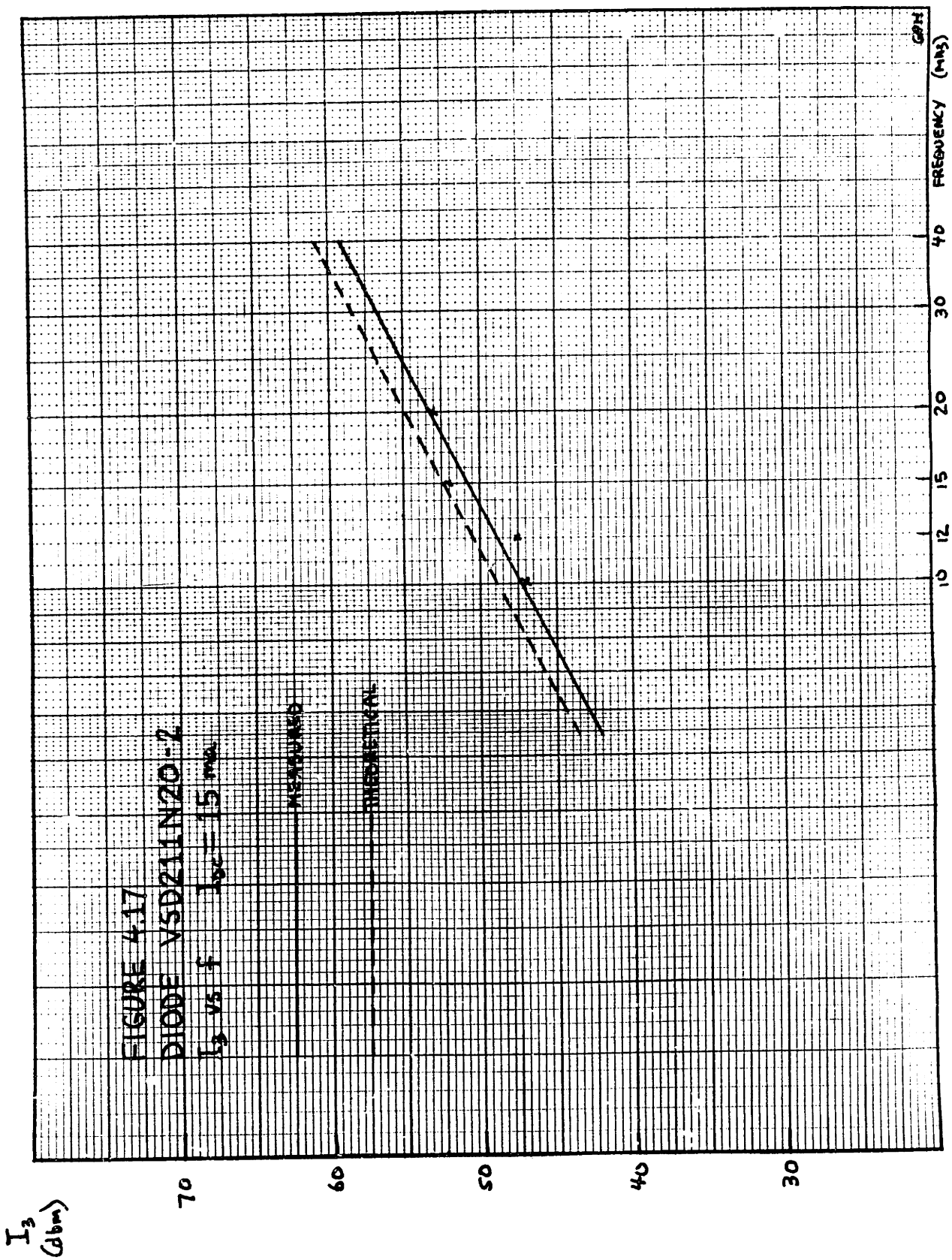
FIGURE 4.17
DIODE VSD211N20-2
I_3 vs f $I_1 = I_2 = 15$ ma
MEASURED
THEORETICAL
I_3 (dbm)
70
60
50
40
30
10
12
15
20
30
40
FREQUENCY (mhz)

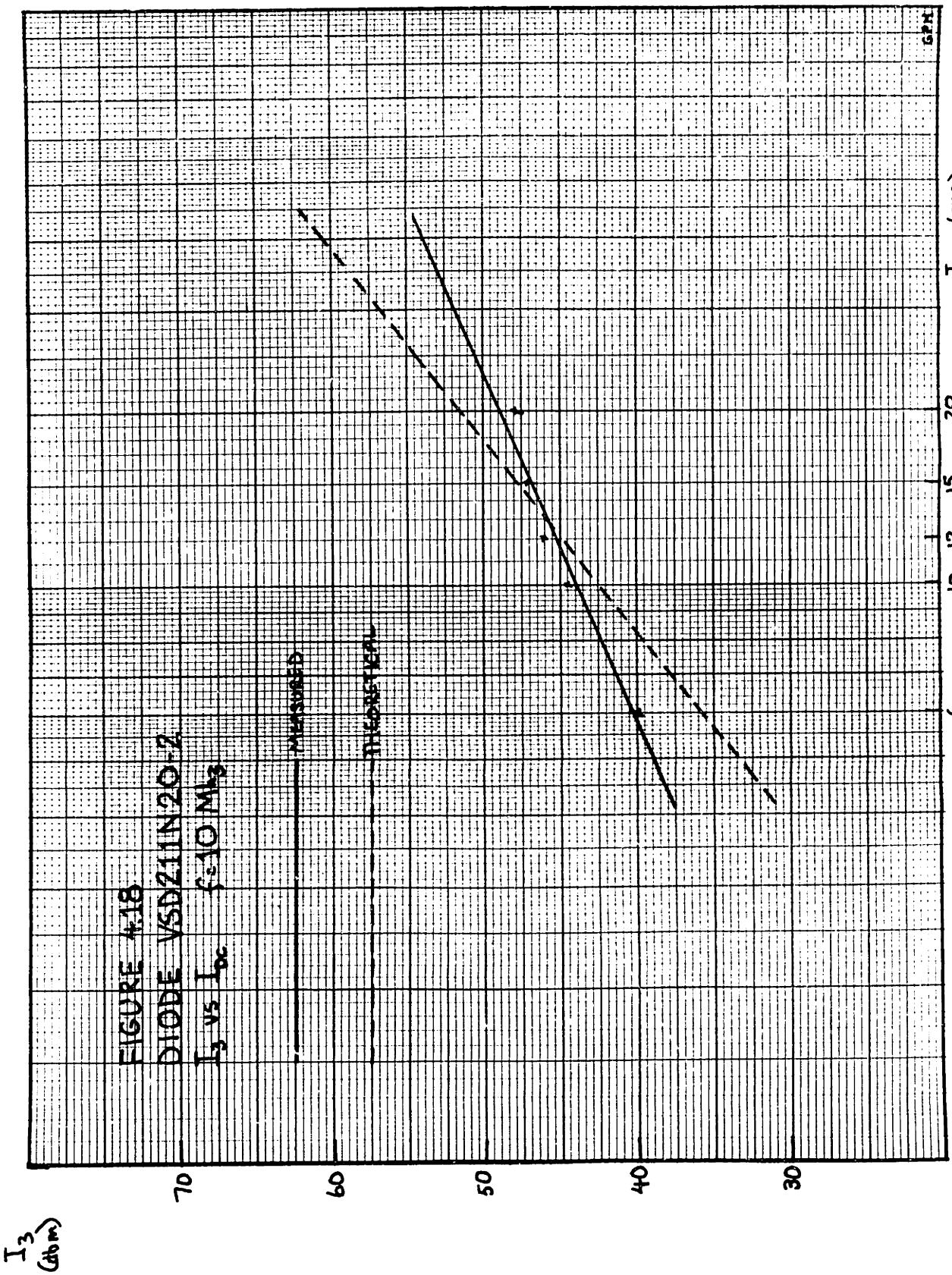
FIGURE 4.18
DIODE VSD211N20-2
I_3 VS I_{DC} f=10 MHz
MEASURED
THEORETICAL
I_3 (ohm)
70
60
50
40
30
I_{DC} (ma)
6
10
12
15
20
GPH

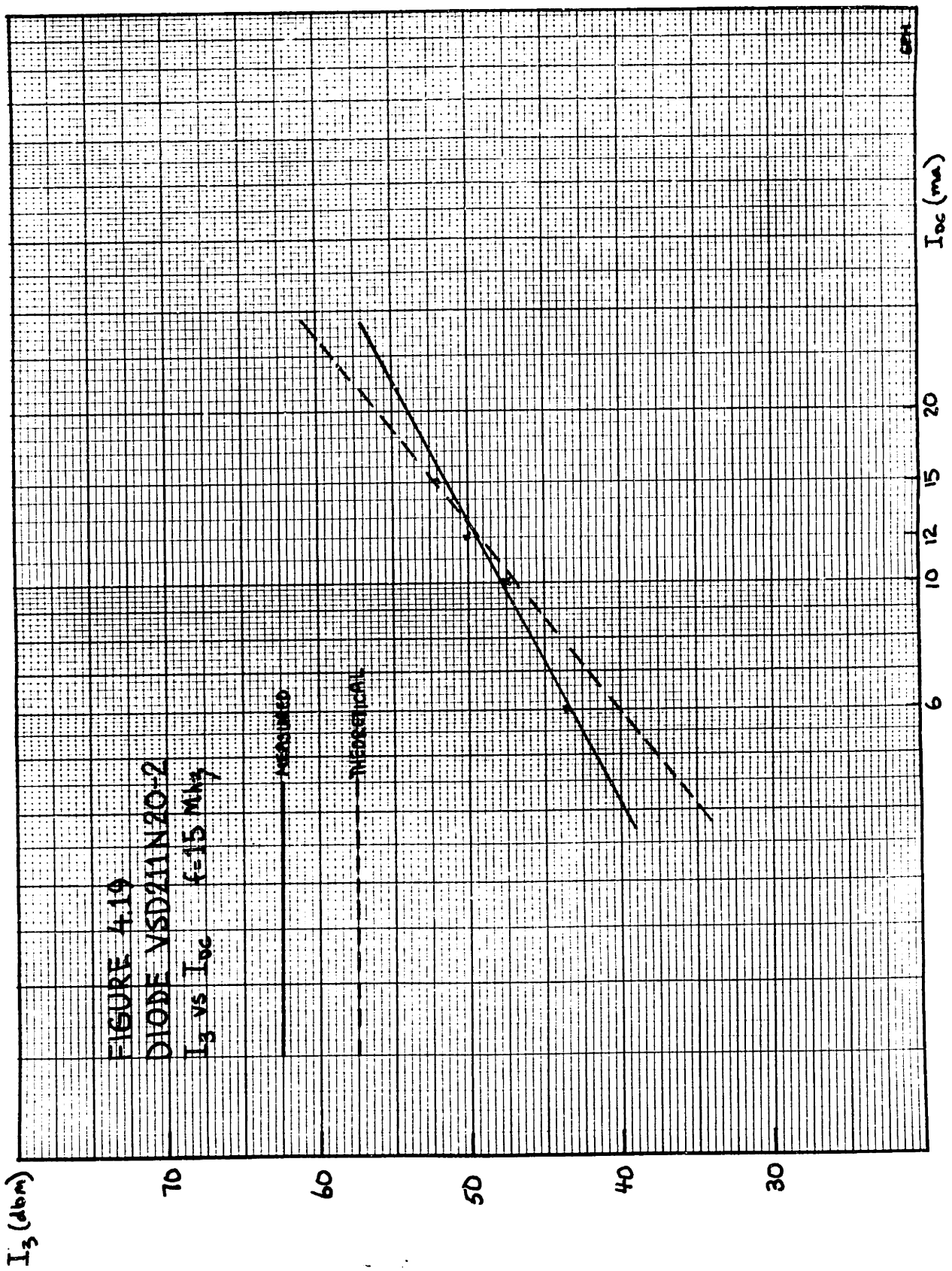
FIGURE 4.19
DIODE VSD211N20-2
I_3 vs I_{DC} f=15 MHz
MEASURED
THEORETICAL
I_3 (dbm)
70
60
50
40
30
6
10
12
15
20
I_{DC} (ma)

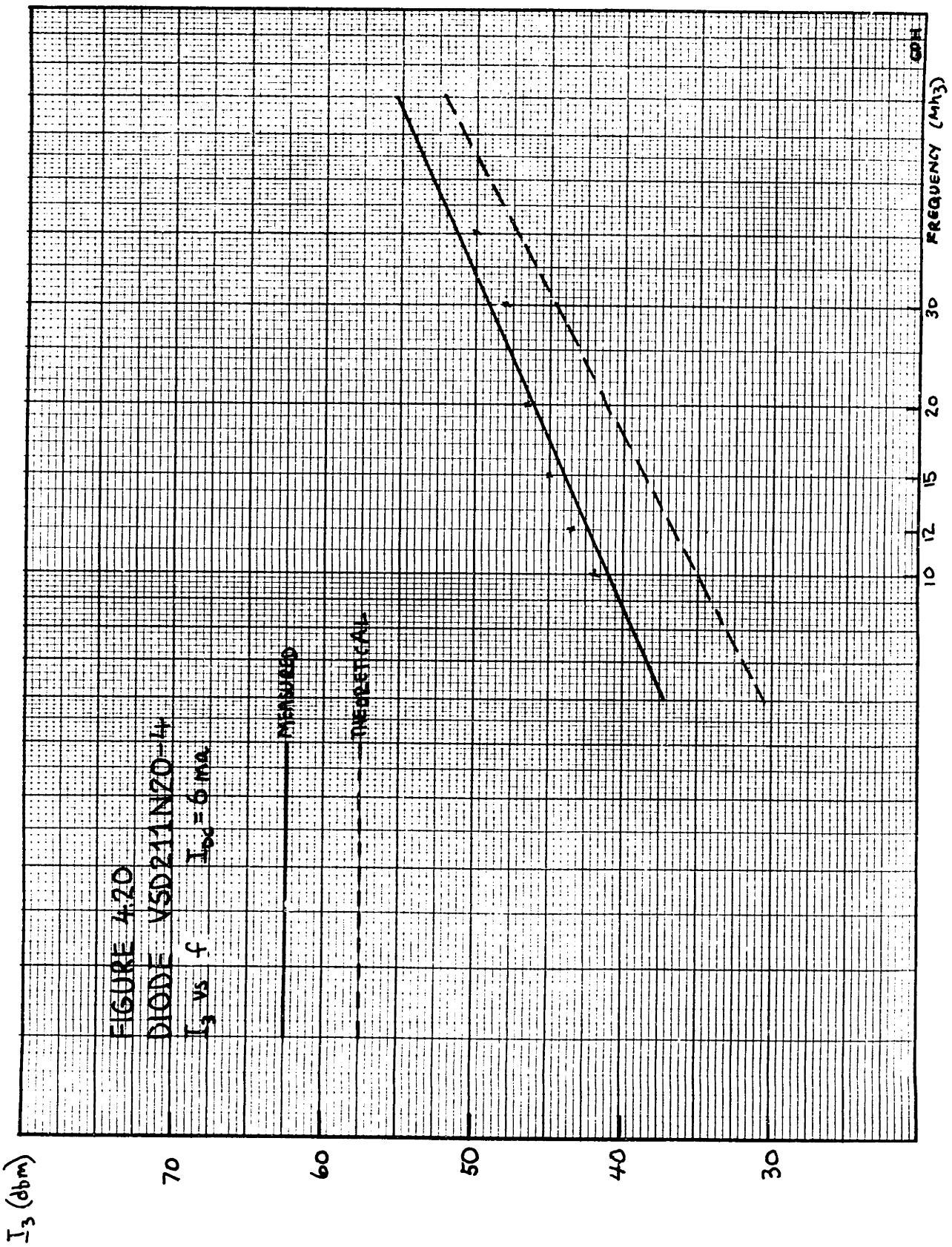
FIGURE 4.20
DIODE VSD211N20-4
I_3 vs f I_{DC} = 6 ma
MEASURED
THEORETICAL
I_3 (dbm)
70
60
50
40
30
10
12
15
20
30
FREQUENCY (MHz)

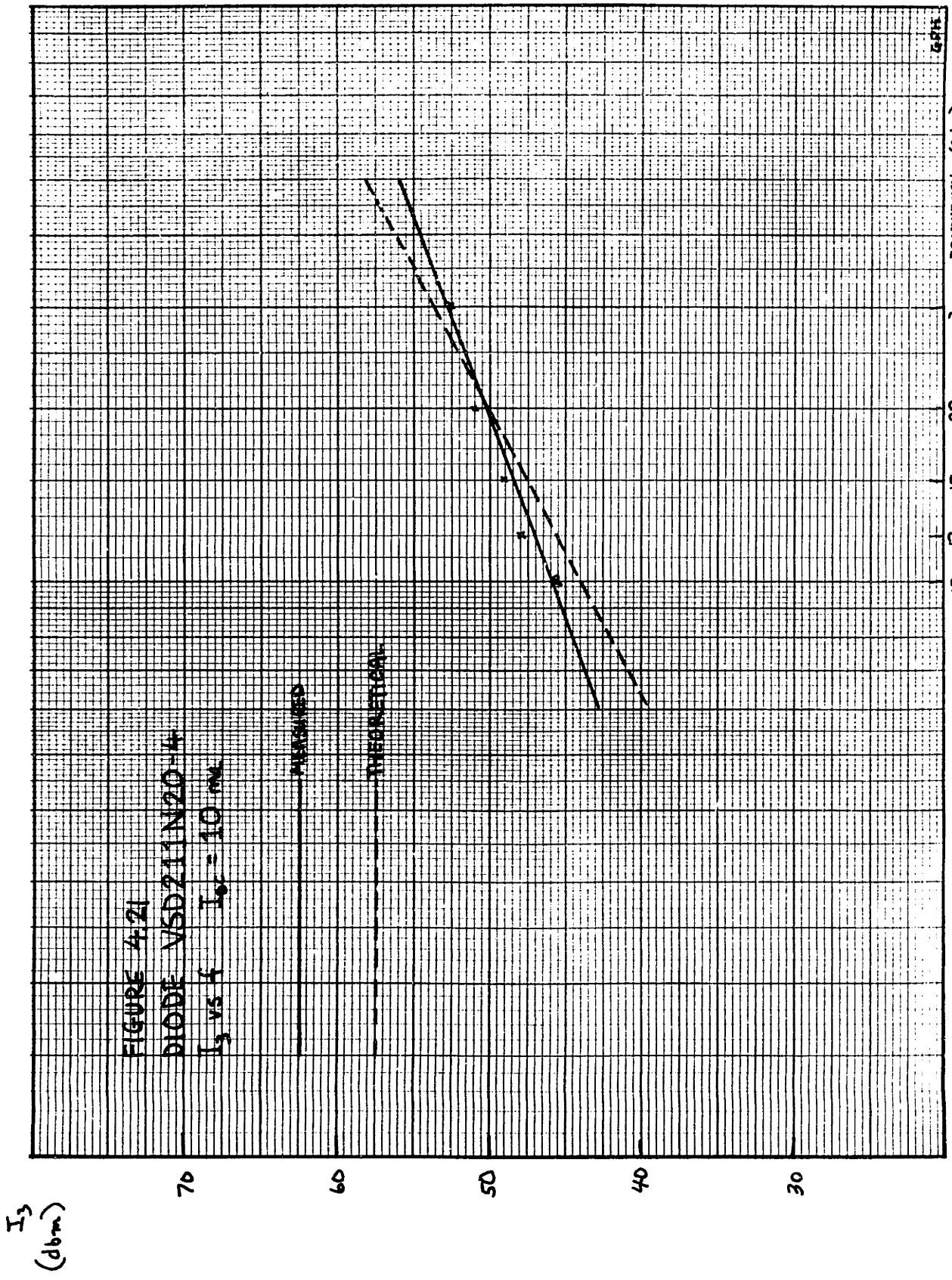
FIGURE 4.21
DIODE VSD211N20-4
I_3 vs f I_0 = 10 mA
MEASURED
THEORETICAL
I_3 (dbm)
70
60
50
40
30
10
12
15
20
30
FREQUENCY (MHz)
GHz

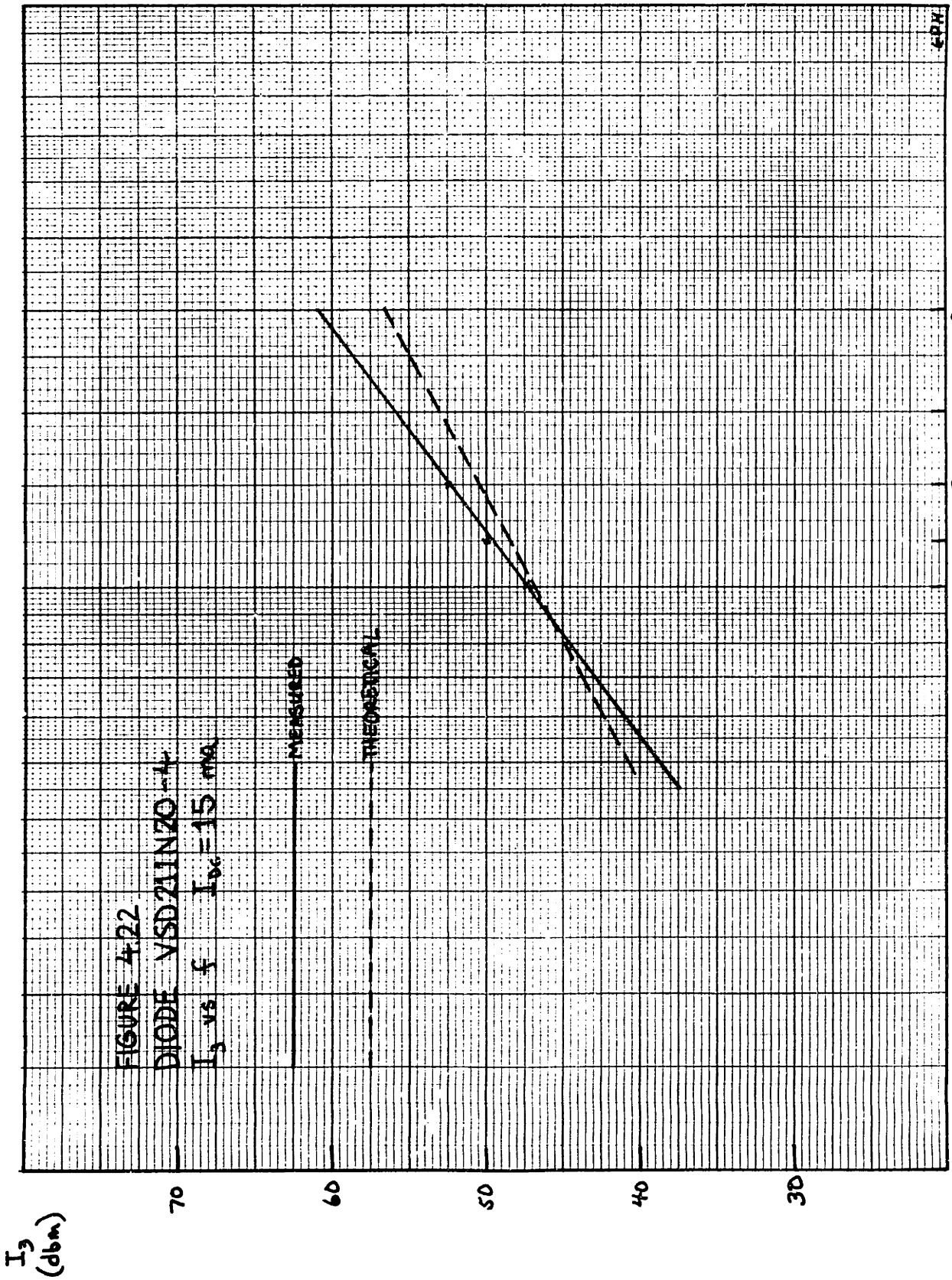
FIGURE 4.22
DIODE VSD2111N20-4
I_3 vs f I_{DC}=15 mA
MEASURED
THEORETICAL
I_3 (dbm)
70
60
50
40
30
10
12
15
20
30
FREQUENCY (MHz)

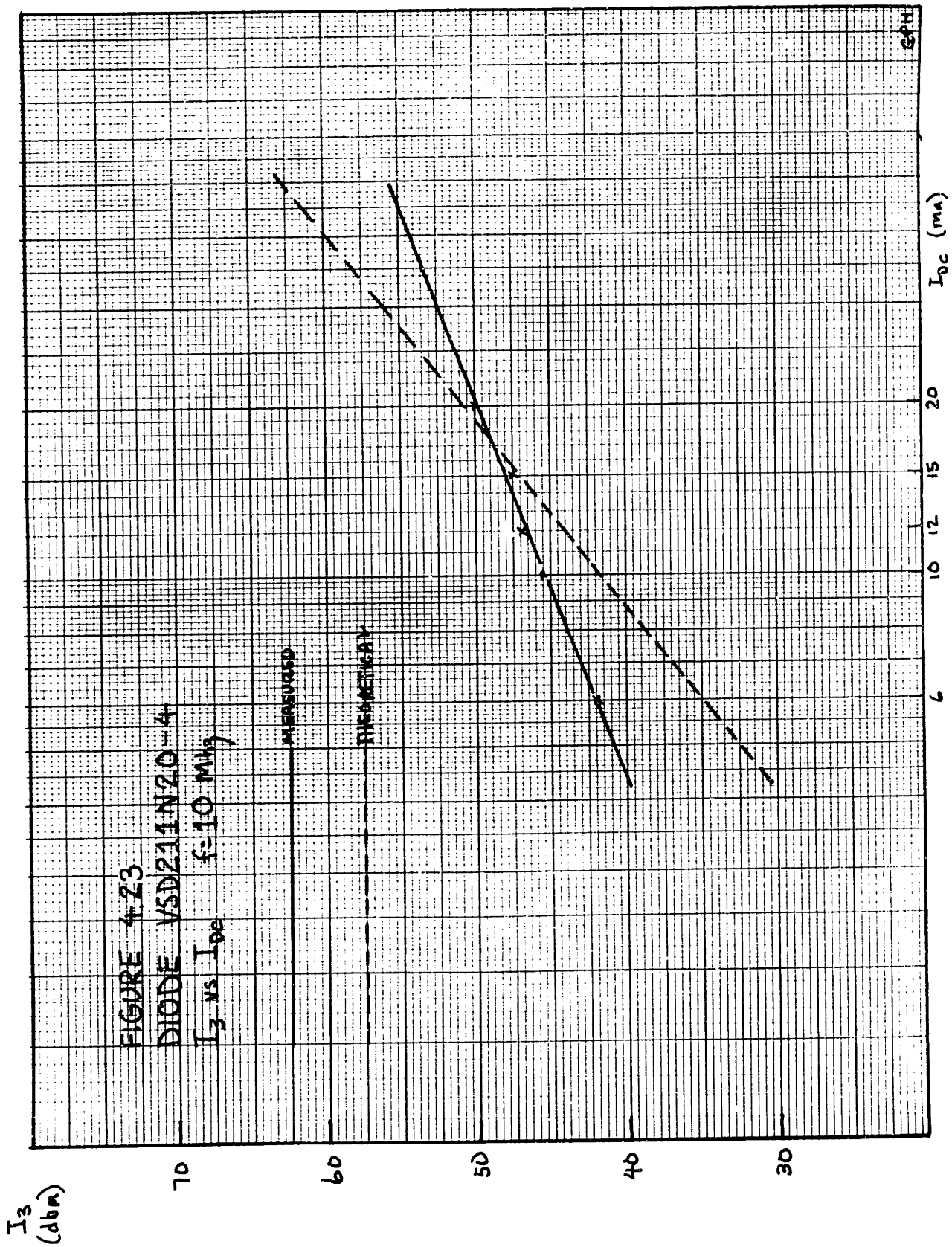
FIGURE 4.23
DIODE 1SD211N2.0-4
I_3 vs I_{DC} f=10 MHz
MEASURED
THEORETICAL
I_3 (dBm)
70
60
50
40
30
I_{DC} (mA)
6
10
12
15
20
GPH

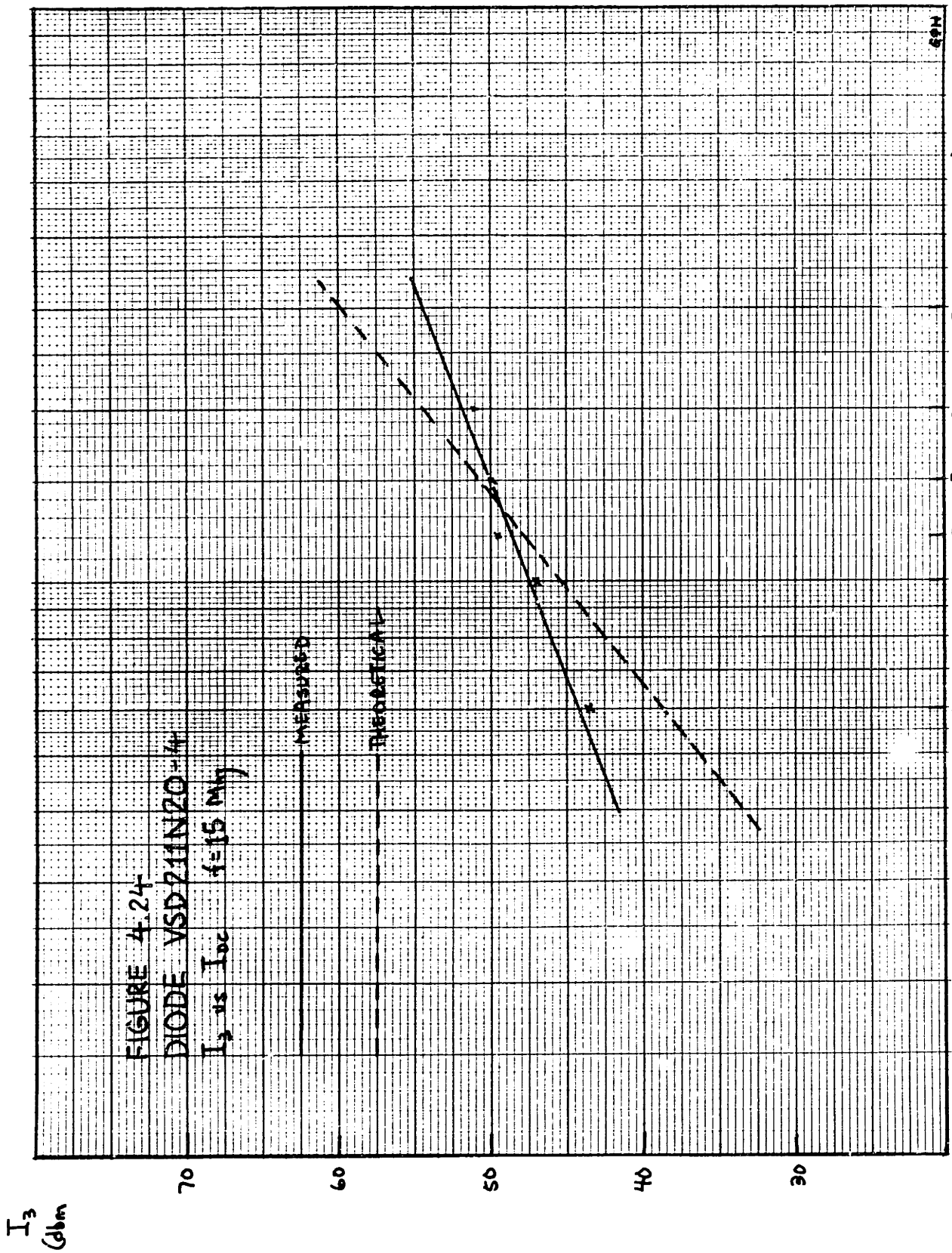
FIGURE 4.24
DIODE VSD211N20-4L
I_3 vs I_{DC} f=15 MHz
MEASURED
THEORETICAL
I_3 dBm
70
60
50
40
30
6
10
12
15
20
30
I_{DC} (mA)

V Conclusion

We have derived the mathematical relationship between harmonic and intermodulation products and the physical device parameters. For minimum distortion products, the I region width should be made as small as possible and the carrier lifetime should be made as large as possible. This will reduce the number of carriers that can recombine in the I region thereby decreasing the intermodulation product level. But in reducing the I region width, one also decreases the power level capabilities - if only the carrier lifetime were increased, power capacity would not be affected. In fact, increasing the carrier lifetime will lead to a more efficient reduction of the distortion products since the i^{th} order distortion product decreases with the $i-1^{th}$ power of the carrier lifetime.

We have not derived in this report, the relationship between current, carrier lifetime and I region width. If such relationships are determined, the PIN diode intercepts can then be fully characterized with respect to current.

Future plans should also include increasing the amount of cancellation possible with the cancellation unit in addition to reducing systems intermodulation levels. In order to further reduce system intermods, larger ferrite cores should be used in the PIN diode mounting circuit and in the hybrids. Also necessary is the stabilization of the PIN diode attenuators in the cancellation unit.

Appendix A Intermodulation Distortion Analysis

Intermodulation distortion, another result of non-linearities in systems, is less desirable than harmonic distortion because some intermodulation products are inband signals and cannot be filtered. In quantatitively analysing intermodulation products we have adopted the following notation introduced by Professor D.H. Steinbrecher [5]:

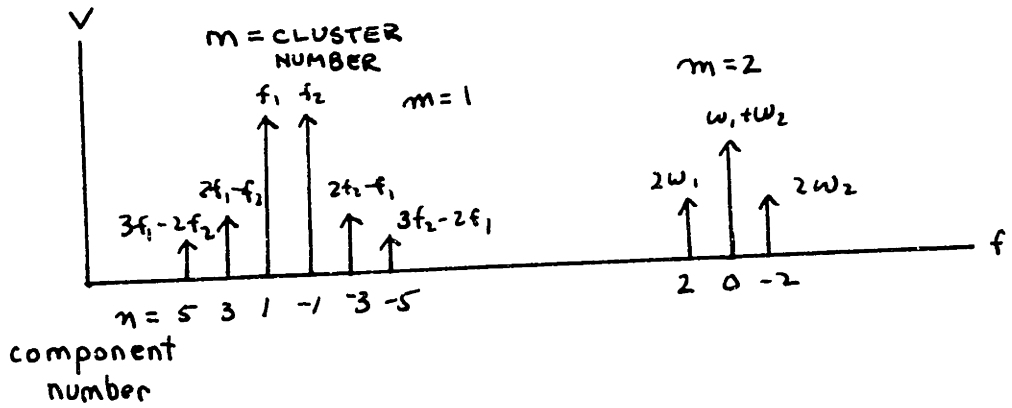

With this notation we can identify any particular cluster by the m index and any component of that cluster by the n index; the frequency of the m,n product is just $f_1 = \left(\frac{m+n}{2}\right) f_1 + \left(\frac{m-n}{2}\right) f_2$ The order of the intermodulation product is $\left|\frac{m+n}{2}\right| + \left|\frac{m-n}{2}\right|$ (In most cases, the most troublesome components are the third order components at $2f_2 - f_1$ and $2f_1 - f_2$)

In analyzing intermodulation products, it is necessary to write the output in a Taylor series expansion:

$$V_o = \sum a_m V_i^n$$

If the input signal is two-tone, then $V_i = (\cos \omega_1 t + \cos \omega_2 t)$ From the above expression it is obvious that some closed expansion for $(\cos \omega_1 t + \cos \omega_2 t)^n$ is necessary. Such an ex-

pression has been derived by Professor D.H. Steinbrecher. [10]

$$(\cos\varphi_1 + \cos\varphi_2)^k = \frac{1}{2^k} \sum_{m=-k}^{k} \sum_{n=-k}^{k} \frac{\left[1 + (-1)^{m+k}\right]}{2} \frac{\left[1 + (-1)^{n+k}\right]}{2} \binom{k}{\frac{k-m}{2}} \binom{k}{\frac{k-n}{2}}$$

$$\cos\left[\frac{m+n}{2}\varphi_1 + \frac{m-n}{2}\varphi_2\right]$$

In describing quantatively the intermodulation products, the intercept form [5] is preferred over the IMR, the intermodulation ratio. The IMR is just the ratio of the third order intermodulation product to the primary signal and thus, a function of the input signal level.

The intercept level is defined as the point wher the n^{th} order intermodulation product level is equal to the primary signal level. This point ifself is a theoretical one and is formed by the projection of the curves in the well behaved region. The well behaved region can be defined as the region where contribution of the i^{th} order product to the $i\text{-}1^{th}$ product is negligible This is equivalent to saying that the slope of the i^{th} order product is i. Using the intercept measure the non-linearities can be characterized without reference to a particular input signal level. See Figure A.2

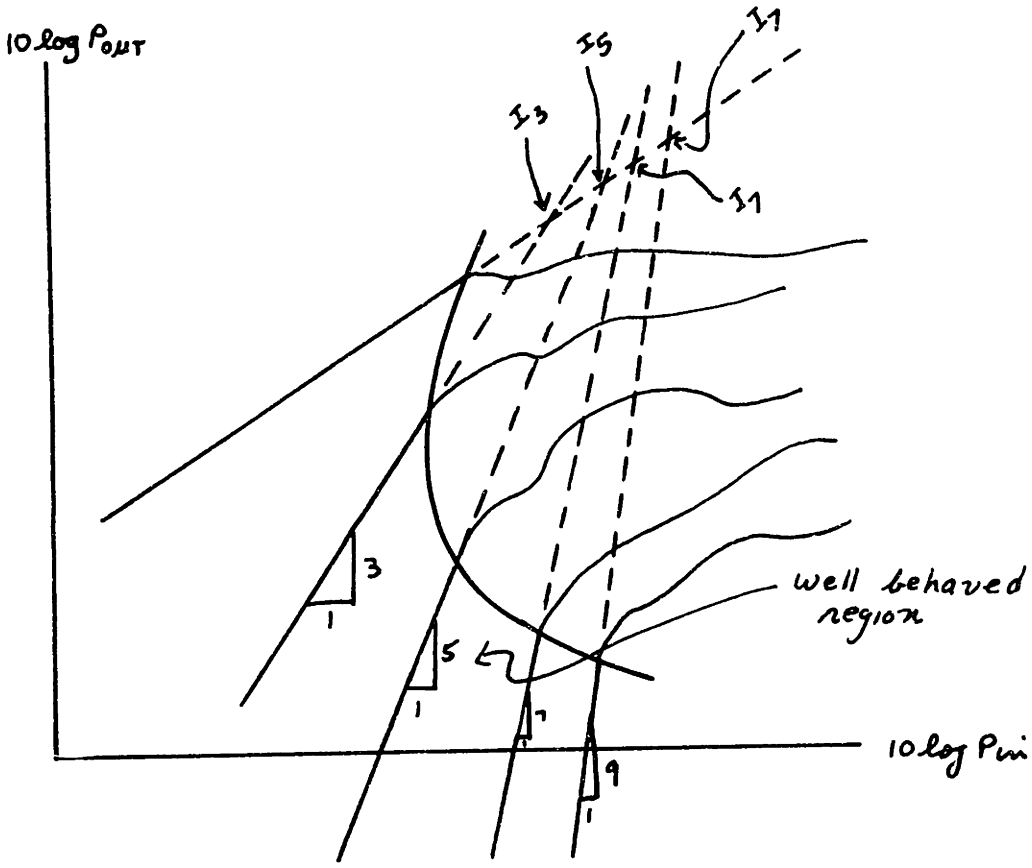

Figure A.2

Appendix B List of Symbols

J	total current density $J = J_e + J_h$
J_e	electron current density
J_h	hole current density
n	electron concentration (equilibrium and intrinsic concentration denoted by o and i respectively)
p	hole concentration (equilibrium and intrinsic concentration denoted by o and i respectively)
N_d	donor concentration
N_a	acceptor concentration
μ_e	electron mobility
μ_h	hole mobility
q	electron charge
E	electric field
k	Boltzmann's constant
T	temperature in degrees Kelvin
b	μ_e/μ_h
D_a	diffusion constant
L_a	diffusion length
τ	carrier lifetime
w	I region width $w = 2d$

References

1. D.E. Fulkerson, The Characterization of the Static Behavior of P-N Junction Devices, IEEE Trans. Electron Devices, ED-14, pp. 385-395, July, 1967.

2. D. Leenov, PIN Diode: AC Impedance at Forward Bias, Bell Telephone Laboratories, Fourth Interim Report on Microwave Solid State Devices, May, 1961.

3. D.A. Kleinman, The Forward Characteristics of the PIN Diode, Bell System Technical Journal, Volume 35, 1956, pp. 685-706.

4. J.P. Curtis and B. Moody, Intermodulation in PIN Diode Switches, Adams Russell Technical Report.

5. R. Mohlere, Intermodulation Distortion Analysis, M.I.T. S.M. thesis, August, 1969.

6. R.N. Hall, Power Rectifiers and Transistors, Proc. IRE, Volume 40, pp. 1512-1518, November, 1952.

7. A. Uhlir, Jr., The Potential of Semiconductor Diodes in High Frequency Communications, Proc. IRE, Volume 46, pp. 1099-1115, 1958.

8. A. Kokkas, private communications

9. P. Chorney, Non-Linearities in the PIN Diode, unpublished paper.

10. D.H. Steinbrecher, 6.628 class notes.

11. H.A. Watson, Microwave Semiconductor Devices and Their Circuit Applications, McGraw-Hill, 1969, pp. 287-290.

Other References

E. Spenke, Notes on the Theory of the Forward Characteristics of Power Rectifiers, Solid State Electronics, 1968 Volume II, pp. 1119-1130.

A. Herlet, The Forward Characteristics of Silicon Power Rectifiers at High Current Densities, Solid State Electronics, 1968, Volume II, pp. 717-742.

H. Benda and E. Spenke, Reverse Recovery Processes in Silicon Power Rectifiers, Proc. IEEE, August, 1967, pp. 1331-1354.

S.C. Choo, Effect of Carrier Lifetime on the Forward Characteristics of High Power Devices, IEEE Transaction on Electron Devices, ED-17, September, 1970.